JOURNAL OF PETROLOGY | VOLUME 48 | NUMBER 12 | PAGES 2261–2287 | 2007 | doi:10.1093/petrology/egm059

Geochemistry, Petrogenesis and Geodynamic Relationships of Miocene Calc-alkaline Volcanic Rocks in the Western Carpathian Arc, Eastern Central Europe

SZABOLCS HARANGI[1]*, HILARY DOWNES[2], MATTHEW THIRLWALL[3] AND KATALIN GMÉLING[4]

[1]DEPARTMENT OF PETROLOGY AND GEOCHEMISTRY, EÖTVÖS UNIVERSITY, BUDAPEST, H-1117, PÁZMÁNY PÉTER SÉTÁNY 1/C, HUNGARY

[2]SCHOOL OF EARTH SCIENCES, BIRKBECK COLLEGE, UNIVERSITY OF LONDON, MALET STREET, LONDON WC1E 7HX, UK

[3]DEPARTMENT OF GEOLOGY, ROYAL HOLLOWAY UNIVERSITY OF LONDON, EGHAM TW20 0EX, UK

[4]DEPARTMENT OF NUCLEAR RESEARCH, INSTITUTE OF ISOTOPES, HUNGARIAN ACADEMY OF SCIENCES, BUDAPEST, HUNGARY

RECEIVED APRIL 14, 2004; ACCEPTED SEPTEMBER 17, 2007
ADVANCE ACCESS PUBLICATION OCTOBER 18, 2007

We report major and trace element abundances and Sr, Nd and Pb isotopic data for Miocene (16·5–11 Ma) calc-alkaline volcanic rocks from the western segment of the Carpathian arc. This volcanic suite consists mostly of andesites and dacites; basalts and basaltic andesites as well as rhyolites are rare and occur only at a late stage. Amphibole fractionation both at high and low pressure played a significant role in magmatic differentiation, accompanied by high-pressure garnet fractionation during the early stages. Sr–Nd–Pb isotopic data indicate a major role for crustal materials in the petrogenesis of the magmas. The parental mafic magmas could have been generated from an enriched mid-ocean ridge basalt (E-MORB)-type mantle source, previously metasomatized by fluids derived from subducted sediment. Initially, the mafic magmas ponded beneath the thick continental crust and initiated melting in the lower crust. Mixing of mafic magmas with silicic melts from metasedimentary lower crust resulted in relatively Al-rich hybrid dacitic magmas, from which almandine could crystallize at high pressure. The amount of crustal involvement in the petrogenesis of the magmas decreased with time as the continental crust thinned. A striking change of mantle source occurred at about 13 Ma. The basaltic magmas generated during the later stages of the calc-alkaline magmatism were derived from a more enriched mantle source, akin to FOZO. An upwelling mantle plume is unlikely to be present in this area; therefore this mantle component probably resides in the heterogeneous upper mantle. Following the calc-alkaline magmatism, alkaline mafic magmas erupted that were also generated from an enriched asthenospheric source. We propose that both types of magmatism were related in some way to lithospheric extension of the Pannonian Basin and that subduction played only an indirect role in generation of the calc-alkaline magmatism. The calc-alkaline magmas were formed during the peak phase of extension by melting of metasomatized, enriched lithospheric mantle and were contaminated by various crustal materials, whereas the alkaline mafic magmas were generated during the post-extensional stage by low-degree melting of the shallow asthenosphere. The western Carpathian volcanic areas provide an example of long-lasting magmatism in which magma compositions changed continuously in response to changing geodynamic setting.

KEY WORDS: *Carpathian–Pannonian region; calc-alkaline magmatism; Sr, Nd and Pb isotopes; subduction; lithospheric extension*

*Corresponding author, Tel: +36-12090555/ext. 8355. Fax: +36-13812108. E-mail: szabolcs.harangi@geology.elte.hu

INTRODUCTION

Calc-alkaline volcanic rocks (andesite–dacite–rhyolite suites) are the typical products of convergent plate margin tectonic settings. They are characterized by enrichment of large ion lithophile elements (LILE) and Pb, but show depletion in high field strength elements (HFSE) causing a negative Nb–Ta anomaly in multielement diagrams (Pearce, 1982; Pearce & Parkinson, 1993). This geochemical signature is commonly explained by the addition of hydrous fluids from subducting oceanic lithosphere combined with the flux of melts from subducted sediments to the mantle wedge, lowering the mantle solidus and leading to magma generation (Gill, 1981; Grove & Kinzler, 1986; Tatsumi, 1989; Hawkesworth *et al.*, 1993; Pearce & Peate, 1995; Elliott *et al.*, 1997; Iwamori, 1998). U-series isotopic studies have shown that melt generation processes beneath volcanic arcs take place on scales of 10^4–10^5 years (Gill & Williams, 1990; Elliott *et al.*, 1997; Thomas *et al.*, 2002; Bourdon *et al.*, 2003; Turner *et al.*, 2006). Thus, it seems reasonable to assume that generation of calc-alkaline magmas is coeval with active subduction. However, it has also been shown that calc-alkaline magmas can be formed by decompression melting of an old subduction-imprinted mantle wedge (Johnson *et al.*, 1978; Cameron *et al.*, 2003) or continental mantle lithosphere previously modified by subduction (Gans *et al.*, 1989; Hawkesworth *et al.*, 1995; Hooper *et al.*, 1995; Wilson *et al.*, 1997; Fan *et al.*, 2003). In both cases, lithospheric extension controls the magma generation whereas the geochemical signature of the magmas is inherited from the older subduction imprint. Thus, calc-alkaline magmatism could also occur without contemporaneous subduction or following cessation of active subduction (post-collisional magmatism).

During Tertiary to Quaternary times, widespread magmatism developed in the Mediterranean and surrounding regions (Wilson & Downes, 1991, 2006; Wilson & Bianchini, 1999; Lustrino, 2000; Harangi *et al.*, 2006; Lustrino & Wilson, 2007). In the Alpine–Mediterranean region, subduction, back-arc extension and lithospheric delamination were accompanied by eruption of a wide range of magma types (Doglioni *et al.*, 1999; Turner *et al.*, 1999; Wilson & Bianchini, 1999; Duggen *et al.*, 2005; Peccerillo, 2005; Harangi *et al.*, 2006). The dominant magma type is calc-alkaline, as would be expected in an orogenic area; however, there is still some debate concerning the interpretation of the petrogenesis of these magmas. In some places, a transition from calc-alkaline to alkaline volcanism is observed (e.g. Betics; Duggen *et al.*, 2003, 2005; North Africa; El Bakkali *et al.*, 1998; Coulon *et al.*, 2002; Sardinia: Lustrino *et al.*, 2007; Western Anatolia; Seyitoğlu & Scott, 1992; Seyitoğlu *et al.*, 1997; Wilson *et al.*, 1997; Aldanmaz *et al.*, 2000; Agostini *et al.*, 2007; Carpathian–Pannonian Region; Szabó *et al.*, 1992; Harangi, 2001; Konečný *et al.*, 2002; Seghedi *et al.*, 2004, 2005), where the composition of the sodic alkaline magmas resembles those that occur in the Alpine foreland (Massif Central, Eifel, Bohemian Massif). This transition is commonly interpreted as a change in the magma source region as a result of changing geodynamic conditions from compression to extension.

In this study, we focus on the northern part of the Carpathian–Pannonian region, where Miocene (16–11 Ma) calc-alkaline magmatism was followed by sodic alkaline magmatism from Late Miocene to Quaternary times (8–0·2 Ma). We present new major and trace element and Sr–Nd–Pb isotopic data for the calc-alkaline volcanic rocks from the western segment of the Carpathian volcanic arc (Fig. 1). This study complements and completes the geochemical dataset for the eastern and northeastern Carpathians (Mason *et al.*, 1996; Seghedi *et al.*, 2001) and we use these internally consistent data to formulate an integrated interpretation of calc-alkaline magmatism in this region. We show that lithospheric extension played a major role in the generation of the calc-alkaline magmatism in the western Carpathians and that subduction had only an indirect influence. An enriched asthenospheric mantle source component, similar to the source of many Tertiary to Quaternary alkaline mafic rocks throughout Europe (Granet *et al.*, 1995; Hoernle *et al.*, 1995; Lustrino & Wilson, 2007), also contributed to the petrogenesis of some of the calc-alkaline magmas of the western Carpathians, together with slab-derived mantle enrichment and mixing with lower crustal materials.

GEOLOGICAL BACKGROUND

The Carpathian–Pannonian Region (CPR) in eastern–central Europe (Fig. 1) comprises an arcuate orogenic belt (the Carpathian arc) and an associated back-arc basin (Pannonian Basin) and has many features in common with Mediterranean-type subduction systems (e.g. Horváth & Berckhemer, 1982; Csontos *et al.*, 1992; Kovac *et al.*, 1998; Fodor *et al.*, 1999; Jolivet *et al.*, 1999; Tari *et al.*, 1999). The main driving force in its evolution was the north–south convergence of the European and African plates. Following Eocene continent–continent collision in the Alps, SSW-dipping subduction continued in the east (Carpathian subduction zone) during the Neogene (Csontos *et al.*, 1992; Nemčok *et al.*, 1998b; Fodor *et al.*, 1999). A consequence of Alpine collision was early Miocene eastward extrusion of a rigid lithospheric block from the Alpine area (Ratschbacher *et al.*, 1991; Csontos *et al.*, 1992; Fodor *et al.*, 1999). This lateral extrusion was made possible by a change from advancing to retreating subduction, providing space for the eastward movement (Royden, 1993). Subduction ceased gradually from west to east along the Carpathian arc from about 15 Ma to 10 Ma, as indicated by migration of the last thrust displacement

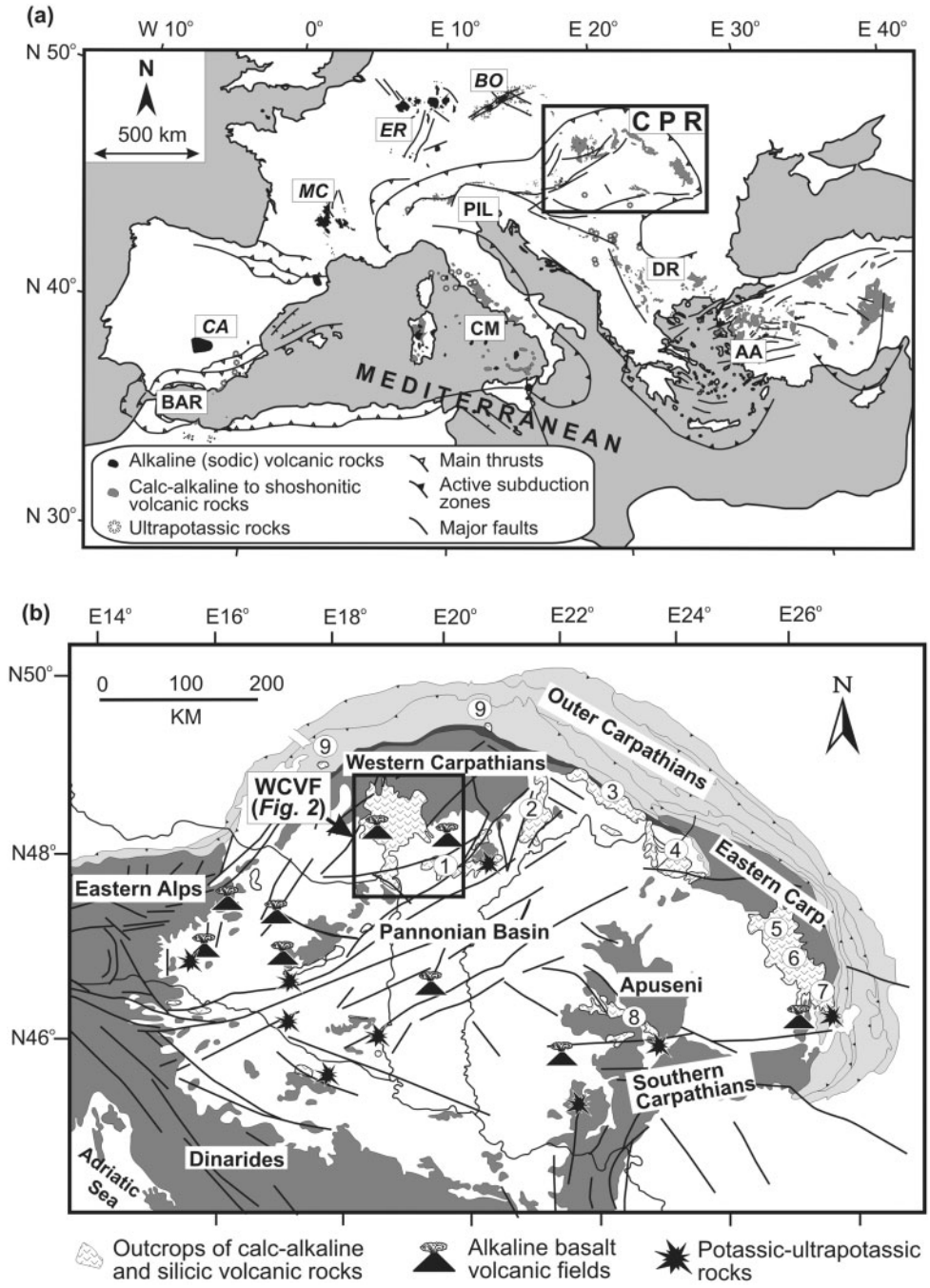

Fig. 1. (a) Position of the Carpathian–Pannonian Region (CPR) within the Mediterranean *sensu lato* orogenic region (after Harangi *et al.*, 2006). Calc-alkaline to shoshonitic volcanic areas: BAR, Betic–Alboran–Rif province; CM, Central Mediterranean; PIL, Periadriatic–Insubric Line; DR, Dinarides and Rhodope; AA, Aegean–Anatolia. Alkaline (sodic) volcanic areas: CA, Calatrava; MC, Massif Central; ER, Eifel–Rhenish volcanic fields; BO, Bohemian volcanic fields. (b) Position of the Western Carpathian Volcanic Field (WCVF) in the Carpathian–Pannonian region. Other calc-alkaline volcanic areas: 1, Cserhát–Mátra; 2, Tokaj–Slanec; 3, Vihorlat; 4, Oas–Gutin, 5, Calimani; 6, Gurghiu; 7, Harghita, 8, Apuseni; 9, dyke swarms in the Outer Carpathians along the Pieniny zone.

and sedimentary depocenters around the Carpathians (Jiříček, 1979; Meulenkamp *et al.*, 1996). Post-collisional slab break-off occurred gradually from west to ESE in a zipper-like process (Tomek & Hall, 1993; Mason *et al.*, 1998; Seghedi *et al.*, 1998; Wortel & Spakman, 2000; Sperner *et al.*, 2002). Slab break-off is thought to be in its final stages beneath the Eastern Carpathians (Vrancea zone), where a still hanging, near-vertical, subducted slab

causes intermediate-depth seismicity (Oncescu *et al.*, 1984; Oncescu & Benjer, 1997; Fan *et al.*, 1998; Sperner *et al.*, 2001, 2004).

Contemporaneously with the retreating subduction, formation of the Pannonian Basin took place during the Middle Miocene (17–12 Ma; Horváth, 1995; Tari *et al.*, 1999), controlled by a combination of eastward lateral extrusion of orogenic blocks, extensional collapse of an overthickened orogenic wedge and the pull of the subducted slab (Csontos *et al.*, 1992; Horváth, 1993; Tari *et al.*, 1999). As a result of this extension, the Pannonian Basin is underlain by thin lithosphere and crust (50–80 km and 22–30 km, respectively; Tari *et al.*, 1999) and is characterized by high heat flow (>80 mW/m^2; Lenkey *et al.*, 2002). The main rifting phase was followed by post-rift thermal subsidence, when several thousand meters of Late Miocene to Quaternary sediments filled parts of the basin. Tectonic inversion has characterized the Pannonian Basin since the Late Pliocene, as a result of the push of the Adriatic plate from the SW and blocking by the East European platform in the east (Horváth & Cloething, 1996).

Seismic tomography images indicate a low-velocity anomaly beneath the CPR (except for the southeastern margin of the Carpathians) to 400 km depth (Spakman, 1990; Wortel & Spakman, 2000). No detached subducted slab has been detected under the western and northeastern parts of the Carpathians. Nevertheless, Tomek & Hall (1993) interpreted deep seismic-reflection data as evidence for subducted European continental crust beneath the Western Carpathians. In contrast, a positive seismic velocity anomaly occurs between the depths of 400 and 600 km beneath the whole region, implying accumulation of relatively cold subducted slab material in the Transition Zone (Spakman, 1990; Wortel & Spakman, 2000; Piromallo *et al.*, 2001).

The complex geodynamics of the CPR resulted in various types of volcanic activity, including repeated explosive eruptions of silicic magmas during the Early to Middle Miocene, extensive calc-alkaline volcanism from the Middle Miocene to the Late Pliocene, and post-extensional alkaline volcanism during the Late Miocene to Quaternary (Szabó *et al.*, 1992; Lexa & Konečný, 1998; Harangi, 2001; Konečný *et al.*, 2002; Seghedi *et al.*, 2004, 2005). Minor potassic and ultrapotassic magmatism took place from Miocene to Quaternary times (Harangi *et al.*, 1995b). Calc-alkaline volcanic complexes occur throughout the CPR, mostly following the thrust belt of the Carpathian arc (Fig. 1b).

The West Carpathian Volcanic Field (WCVF) is defined here as forming the westernmost part of this volcanic chain on the northern edge of the Pannonian Basin. It consists of erosional remnants of the volcanic complexes of the Visegrád Mts, Börzsöny and central Slovakia (Konečný *et al.*, 1995; Harangi *et al.*, 1999; Karátson *et al.*, 2000, 2007). To the east, the volcanic chain continues with the Miocene Cserhát and Mátra volcanoes, whereas to the north, sporadic dyke swarms occur in the Pieniny zone of the Outer Carpathians (Birkenmajer *et al.*, 2000; Trua *et al.*, 2006).

The WCVF calc-alkaline magmas erupted in both terrestrial and shallow marine environments (Konečný *et al.*, 1995; Karátson *et al.*, 2000), forming composite volcanoes with effusive and extrusive rocks associated with pyroclastic and epiclastic breccias (Karátson, 1995; Konečný *et al.*, 1995; Karátson *et al.*, 2000, 2007). Volcanic activity commenced at 16–16·5 Ma with eruption of garnet-bearing andesitic to rhyodacitic magmas (Harangi *et al.*, 2001), followed by andesites and dacites. It peaked at 14–15 Ma, when several andesitic stratovolcanic and lava dome complexes were formed. Structural and palaeomagnetic analyses indicate syn-volcanic extension tectonics (Nemčok & Lexa, 1990; Nemčok *et al.*, 1998a) and significant block rotation events (Karátson *et al.*, 2000, 2007). In the south (Börzsöny and Visegrád Mts), volcanism terminated at 14 Ma, whereas in central Slovakia it lasted until 11 Ma (Konečny *et al.*, 1995, 2002).

After a few million years of quiescence, volcanism renewed with development of sporadic alkaline basaltic volcanoes within central Slovakia (8–6 Ma), followed by a more intense alkaline basaltic volcanism in the Nógrád–Gemer Volcanic Field (NGVF, Fig. 2; Dobosi *et al.*, 1995). The last volcanic eruption in this area occurred about 130–150 kyr ago (Simon & Halouzka, 1996).

The andesites and dacites are usually crystal-rich. Disequilibrium textural and compositional features in the phenocryst assemblage suggest complex magmatic evolution. In some localities, xenoliths are particularly abundant, representing both shallow subvolcanic crustal lithologies and cognate magmatic inclusions. In general, a gradual change of phenocryst assemblage is observed in the andesites. Early stage (16·5–15 Ma) andesites typically contain hornblende and sometimes also biotite, whereas the younger (15–13 Ma) rocks are mostly two-pyroxene andesites. Differentiated rocks include sporadic early-stage rhyodacites (16·5 Ma) in the Visegrád Mts (Harangi *et al.*, 2001) and late-stage rhyolites (11–12·5 Ma) as well as subvolcanic granodiorite and diorite bodies in central Slovakia (Konečný *et al.*, 1995). The 16·5 Ma rhyodacites contain plagioclase and biotite phenocrysts in addition to garnet, whereas the late-stage rhyolites are also characterized by the dominance of plagioclase and biotite, but lack garnet. Sanidine and quartz phenocrysts occur subordinately in the rhyolites. Calc-alkaline volcanism in the WCVF terminated with eruption of small-volume high-alumina basalts and basaltic andesites in the northern part at 11 Ma. These rocks contain olivine, clinopyroxene and plagioclase phenocrysts.

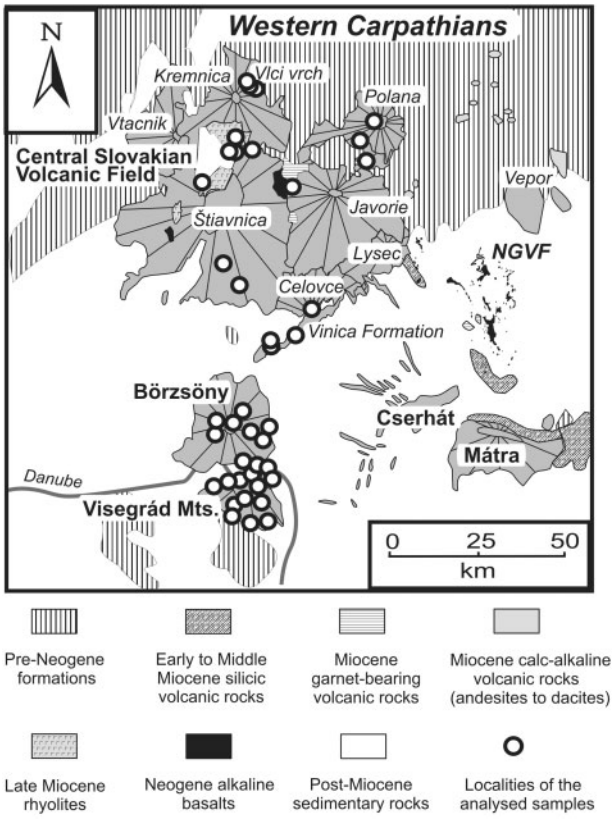

Fig. 2. Simplified geological map of the Western Carpathian Volcanic Field (consisting of the stratovolcanic complexes of central Slovakia and the stratovolcanoes of Börzsöny and the Visegrád Mts) showing the localities of the studied samples. NGVF, Nógrád–Gömör Volcanic Field, comprising Late Miocene to Quaternary alkaline basaltic volcanoes.

SAMPLING AND ANALYTICAL TECHNIQUES

Over 100 fresh samples of volcanic rocks were collected from various sample localities covering the entire WCVF (Fig. 2). All of the samples were analysed for major and trace elements and for Sr isotope ratios. Based on these data, a smaller number of samples were selected for determination of the rare earth element (REE) contents and Nd and Pb isotope ratios. Salters *et al.* (1988) published the first Nd–Sr–Pb isotope data for some Miocene calc-alkaline volcanic rocks from the northern part of the Pannonian Basin. In this paper, we use their data from three WCVF samples (55, 57 and 107 from Börzsöny) for comparison.

The major and trace element characteristics of representative samples are presented in Table 1; the complete dataset can be downloaded from the *Journal of Petrology* website (http://www.petrology.oxfordjournals.org/). Major and trace element compositions were determined using a Philips PW1480 X-ray fluorescence spectrometer at Royal Holloway University of London (RHUL) using fused glass discs (for major elements) and pressed powder pellets (for trace elements). Details of analytical reproducibility have been given by Baker *et al.* (1997). Rare earth elements (REE) were analysed by inductively coupled plasma-atomic emission spectroscopy (ICP-AES) at RHUL using the method described by Walsh *et al.* (1981). The boron concentrations of whole rock samples were measured by the cold neutron prompt gamma neutron activation analysis (PGNAA) facility at the Budapest Research Reactor, Hungary, with conditions described in detail by Gméling *et al.* (2005).

Whole-rock Sr and Nd isotopic compositions were determined at RHUL. Sample powders were leached in hot 6M HCl for 1 h to remove any effects of post-magmatic groundmass alteration. Sr and Nd were extracted by conventional ion exchange techniques, and their isotope ratios were determined by thermal ionization mass spectrometry (TIMS) on a five-collector VG-354 system in multidynamic mode as described by Thirlwall (1991). $^{87}Sr/^{86}Sr$ was normalized to $^{86}Sr/^{88}Sr = 0{\cdot}1194$ and $^{143}Nd/^{144}Nd$ to $^{146}Nd/^{144}Nd = 0{\cdot}7219$. An in-house laboratory Nd standard (Aldrich) yielded $^{143}Nd/^{144}Nd = 0{\cdot}511412 \pm 5$ (2SD on eight analyses; equivalent to 0·511847 for the international standard La Jolla) and SRM987 gave $^{87}Sr/^{86}Sr = 0{\cdot}710241 \pm 16$ (2SD on 16 analyses). The measured Sr isotope values (Table 2) were age-corrected but this resulted in little change in the $^{87}Sr/^{86}Sr$ ratios. Reported Nd isotope ratios are uncorrected as the age correction would be too small to affect the measured ratios. Pb isotope analysis was carried out using a $^{207}Pb/^{204}Pb$ double-spike method described, together with chemical separation and loading techniques, by Thirlwall (2000). The Pb isotope ratios were determined partly by TIMS and partly by multicollector-ICP-mass spectrometry (MC-ICP-MS) at RHUL. Seven of the analysed samples were measured by both techniques, yielding the same results within the analytical uncertainty. Reproducibility of the SRM981 standard during the period of analysis is given by Thirlwall (2000).

GEOCHEMISTRY

Major and trace element data

The WCVF volcanic rocks show a range of SiO_2 contents from 49 to 78 wt %, although they are dominantly andesites (SiO_2 57–63 wt %). The most mafic rocks and rhyolites occur only in Central Slovakia and belong only to the latest stage of magmatism. The calc-alkaline mafic rocks (SiO_2 49–57 wt %; MgO >3 wt %) have Mg-numbers [$= Mg/(Mg + Fe^{2+})$, where Fe^{2+} is estimated assuming $FeO/(FeO + Fe_2O_3) = 0{\cdot}55$] of 0·5–0·6, suggesting variable degrees of crystal fractionation. On the SiO_2 vs K_2O diagram (Fig. 3a), the WCVF rocks plot mostly along the boundary between the medium-K and high-K calc-alkaline series, although rhyolites from Central

Table 1: Major and trace element composition of the calc-alkaline volcanic rocks from the WCVF

	Börzsöny					Visegrád Mts					
Locality:	Kis-Kelemen hill	Hegyes hill	Nagy-hideg hill	Szarvas-kő	Nagy-Mána hill	Peres hill	Hold-világ creek	Malom valley	Gyopár spring	Kis-Csikóvár hill	Dobo-gókő
Sample:	B7L	B-72	B-3	B-134	B-144	PS5	H2	L2	CS1	CS3A	12/1A
Major elements (wt %)											
SiO_2	62·10	56·86	56·41	59·14	57·75	69·63	60·33	60·26	60·69	59·09	53·15
TiO_2	0·62	0·89	0·92	0·81	0·75	0·27	0·71	0·65	0·79	0·71	0·76
Al_2O_3	18·69	18·17	18·53	18·35	18·82	16·25	18·30	17·90	18·05	18·28	19·05
Fe_2O_3	5·00	8·23	8·19	6·41	7·43	3·04	6·81	6·50	6·70	7·08	8·76
MnO	0·07	0·17	0·17	0·11	0·12	0·07	0·09	0·07	0·12	0·13	0·17
MgO	1·64	2·78	3·17	2·52	2·83	0·56	1·84	2·81	2·14	2·53	5·11
CaO	6·52	7·18	7·75	6·89	6·78	3·62	6·67	6·16	6·53	6·98	9·43
Na_2O	3·10	2·66	3·13	3·15	2·89	3·54	2·95	2·86	2·44	2·86	2·16
K_2O	2·06	2·45	1·77	2·07	2·26	2·61	2·01	2·13	2·00	1·80	1·23
P_2O_5	0·15	0·21	0·23	0·18	0·20	0·14	0·17	0·16	0·19	0·16	0·11
Total	99·95	99·60	100·27	99·63	99·83	99·73	99·88	99·50	99·65	99·62	99·93
LOI	0·47	0·86	0·48	0·34	0·53	0·67	0·71	0·96	0·76	0·80	1·78
Trace elements (ppm)											
B	n.a.	29·80	12·30	10·90	21·20	n.a.	11·10	13·40	7·20	15·80	15·30
Ni	7	5	14	9	7	5	10	8	5	7	11
Cr	14	12	40	26	17	5	18	24	9	13	23
V	113	138	146	141	90	20	124	107	54	137	226
Sc	17·00	19·50	19·10	20·60	19·30	5·10	18·40	18·50	12·30	18·70	32·00
Rb	76	86	70	73	95	100	74	81	63	63	45
Ba	528	912	549	497	574	502	537	448	792	469	319
Pb	18·4	29·3	13·5	16·1	21·8	29·0	16·9	16·8	25·2	17·8	13·8
Sr	363	475	427	373	434	289	339	317	473	342	419
Zr	124	147	145	151	148	139	137	130	193	130	68
Nb	9	9	8	8	9	9	9	8	16	8	8
Y	18	30	29	23	24	13	24	20	25	23	20
Th	10·40	13·00	8·00	9·30	11·00	10·70	9·00	8·90	13·20	8·50	6·70
La	26·80	33·01	22·11	24·80	28·50	30·40	25·30	23·01	42·01	23·30	30·14
Ce	47·30	63·56	47·03	46·10	54·10	54·00	48·70	47·86	84·76	47·00	38·27
Nd	20·70	26·20	21·80	21·70	24·30	20·30	22·50	19·10	32·50	21·00	18·63
Sm	n.a.	5·26	4·65	n.a.	n.a.	n.a.	n.a.	3·83	6·01	n.a.	n.a.
Eu	n.a.	1·44	1·39	n.a.	n.a.	n.a.	n.a.	1·10	1·52	n.a.	1·09
Gd	n.a.	5·48	5·01	n.a.	n.a.	n.a.	n.a.	3·75	5·53	n.a.	n.a.
Dy	n.a.	5·11	4·85	n.a.	n.a.	n.a.	n.a.	3·33	4·29	n.a.	n.a.
Ho	n.a.	1·04	0·99	n.a.	n.a.	n.a.	n.a.	0·65	0·78	n.a.	n.a.
Er	n.a.	2·64	2·56	n.a.	n.a.	n.a.	n.a.	1·61	1·66	n.a.	n.a.
Yb	n.a.	2·96	2·86	n.a.	n.a.	n.a.	n.a.	1·84	1·68	n.a.	1·42
Lu	n.a.	0·49	0·48	n.a.	n.a.	n.a.	n.a.	0·31	0·27	n.a.	0·21

(continued)

Table 1: Continued

	Visegrád Mts						Central Slovakia				
Locality:	Prédiká-lószék	Apátkút valley	Szamár hill	Hideg-lelós	Dömör-kapu	Prépost hill	Hrusov	Celovce quarry	Pol'ana SW	Rochy W	Ladzany
Sample:	30/1	A7	S3b	S4	12/2A	PR1	S-V1	S-V4	S-P4	S-P5	SK3
Major elements (wt %)											
SiO_2	59·06	59·89	55·46	56·80	56·68	54·93	57·13	58·05	59·03	57·18	59·36
TiO_2	0·58	0·60	0·83	0·75	0·90	0·81	0·83	0·88	0·82	1·10	0·78
Al_2O_3	18·05	18·13	19·02	18·57	17·94	18·91	17·21	16·79	17·53	17·50	18·02
Fe_2O_3	6·48	6·84	7·99	7·87	7·60	7·73	7·53	7·23	7·39	8·33	7·09
MnO	0·12	0·10	0·11	0·12	0·12	0·12	0·12	0·13	0·13	0·16	0·14
MgO	3·23	2·52	3·40	3·45	4·06	4·19	4·63	4·66	3·13	2·96	3·21
CaO	7·35	5·99	8·47	7·66	7·80	8·51	8·02	7·26	6·32	6·96	6·56
Na_2O	2·88	2·97	2·78	2·83	2·26	2·97	2·72	2·18	2·81	2·93	2·90
K_2O	1·93	2·33	1·67	1·84	1·97	1·68	1·58	2·36	2·11	2·00	1·69
P_2O_5	0·16	0·24	0·14	0·14	0·16	0·14	0·12	0·13	0·22	0·22	0·13
Total	99·84	99·61	99·87	100·03	99·49	99·99	99·89	99·67	99·49	99·34	99·88
LOI	1·13	1·47	1·03	0·54	0·37	0·27	0·72	0·86	0·41	0·45	0·41
Trace elements (ppm)											
B	n.a.	n.a.	15·30	18·20	12·70	16·70	19·70	24·80	11·20	16·00	31·90
Ni	9	13	12	6	11	10	49	8	5	5	6
Cr	24	35	20	11	48	15	165	56	13	10	14
V	128	108	188	160	189	194	173	171	159	182	127
Sc	20·60	17·30	26·20	20·50	30·20	25·10	27·80	28·90	23·20	20·70	22·00
Rb	76	86	58	70	59	50	55	69	78	70	59
Ba	551	658	437	424	707	418	311	438	505	368	385
Pb	20·0	23·5	17·7	9·9	17·2	17·4	9·8	12·1	10·4	9·0	8·4
Sr	414	473	375	321	489	396	264	275	354	342	259
Zr	105	142	124	135	183	117	123	167	141	145	146
Nb	8	11	9	9	13	9	9	11	18	15	9
Y	17	21	22	22	29	21	22	26	24	28	26
Th	11·00	14·10	6·80	7·20	11·60	6·70	6·10	8·40	9·30	6·60	7·30
La	28·10	39·30	20·80	20·91	37·73	18·71	17·82	23·91	32·90	24·51	22·11
Ce	52·13	71·40	40·60	44·54	73·92	39·19	38·16	51·84	58·50	51·66	46·83
Nd	18·50	29·60	19·20	18·40	29·70	17·20	17·00	22·50	26·30	23·30	19·30
Sm	3·46	n.a.	n.a.	3·81	5·50	3·52	3·48	4·57	n.a.	4·92	3·94
Eu	1·02	n.a.	n.a.	1·08	1·39	1·08	1·01	1·25	n.a.	1·41	1·13
Gd	3·33	n.a.	n.a.	3·93	5·51	3·69	3·71	4·64	n.a.	5·23	4·23
Dy	2·91	n.a.	n.a.	3·71	4·79	3·51	3·64	4·42	n.a.	4·83	4·22
Ho	0·57	n.a.	n.a.	0·74	0·97	0·70	0·73	0·89	n.a.	0·97	0·87
Er	1·41	n.a.	n.a.	1·89	2·41	1·77	1·85	2·29	n.a.	2·45	2·30
Yb	1·63	n.a.	n.a.	2·09	2·59	1·93	2·01	2·57	n.a.	2·66	2·64
Lu	0·27	n.a.	n.a.	0·34	0·43	0·31	0·33	0·43	n.a.	0·44	0·44

(continued)

Table 1: Continued

	Central Slovakia									
Locality:	Hlinik	Kyslinki, Pol'ana	Ihrac	Bodan	Stara Kremnica	Stara Kremnica	Vlci vrch	Vlci vrch	Vlci vrch	Ziar nad Hronom
Sample:	SK9	S-P1	SK4	SK2	SK6	SK7	SK5	ba4(III)	di2(E)	SK8
Major elements (wt %)										
SiO_2	73·88	68·28	64·48	66·37	77·86	75·18	52·31	50·52	54·68	51·74
TiO_2	0·21	0·33	0·59	0·81	0·11	0·11	1·00	1·01	0·82	1·16
Al_2O_3	13·62	15·49	16·39	15·41	12·75	13·14	18·15	16·92	17·34	17·84
Fe_2O_3	1·80	4·00	4·27	5·68	1·91	1·49	9·14	11·38	7·83	10·05
MnO	0·05	0·09	0·15	0·05	0·02	0·07	0·16	0·2	0·13	0·18
MgO	0·33	1·48	2·02	0·58	0·16	0·18	4·38	5·67	3·72	4·90
CaO	1·38	3·79	4·87	3·22	0·53	1·10	8·94	9·52	7·52	9·25
Na_2O	2·49	2·75	2·70	3·86	1·95	2·86	3·26	2·71	3·09	2·91
K_2O	5·64	2·73	3·81	3·56	4·58	5·37	1·70	1·36	2·28	1·55
P_2O_5	0·05	0·14	0·30	0·23	0·03	0·03	0·59	0·49	0·57	0·31
Total	99·45	99·08	99·58	99·77	99·90	99·53	99·63	99·78	97·98	99·89
LOI	3·15	3·19	2·47	1·08	2·01	3·43	0·00	0·1	1·6	1·78
Trace elements (ppm)										
B	50·80	4·40	52·40	22·10	35·20	75·90	8·80	3·88	11·66	8·60
Ni	4	5	8	3	4	4	11	20	20	10
Cr	5	9	11	4	3	3	23	n.a.	n.a.	17
V	18	56	102	48	10	8	208	227	161	195
Sc	4·10	10·70	13·20	18·40	1·30	2·20	21·00	28	17	25·30
Rb	207	103	135	133	183	191	55	44	92·1	46
Ba	707	522	888	710	694	764	696	467·3	810·7	454
Pb	24·8	17·6	18·4	16·5	28·5	27·6	7·3	n.a.	n.a.	8·2
Sr	139	293	455	229	89	149	693	576·4	660·6	452
Zr	166	109	169	273	116	121	151	119·1	158·2	146
Nb	26	15	47	26	35	42	61	37·7	57·4	21
Y	20	14	19	31	13	13	30	26·8	26·6	28
Th	28·40	10·40	21·70	16·20	33·80	34·10	10·50	7·1	16	4·70
La	43·01	29·70	45·11	41·23	68·50	47·90	53·11	37·6	57·2	24·41
Ce	77·49	51·80	80·10	83·78	75·60	76·41	100·53	82·4	118·5	51·93
Nd	22·70	19·20	25·10	33·50	26·00	18·00	41·00	34·6	41·6	23·10
Sm	3·76	n.a.	4·05	6·35	n.a.	2·56	7·09	5·8	6·9	4·72
Eu	0·61	n.a.	1·14	1·56	n.a.	0·51	1·99	1·73	1·69	1·42
Gd	3·22	n.a.	3·61	6·20	n.a.	2·05	6·47	5·13	5·3	4·98
Dy	2·88	n.a.	3·03	5·43	n.a.	1·89	5·28	4·39	4·75	4·72
Ho	0·57	n.a.	0·60	1·07	n.a.	0·39	1·04	0·98	0·96	0·95
Er	1·42	n.a.	1·44	2·65	n.a.	0·96	2·45	2·56	2·72	2·40
Yb	1·85	n.a.	1·74	2·80	n.a.	1·41	2·66	2·35	2·52	2·59
Lu	0·31	n.a.	0·29	0·45	n.a.	0·25	0·43	0·34	0·37	0·42

Composition of the early stage garnet-bearing andesites to rhyodacites has been given by Harangi *et al*. (2001). LOI, loss on ignition; n.a., not analysed.

Table 2: Sr, Nd, Pb isotope composition of the calc-alkaline volcanic rocks from the WCVF

Sample	Rock type	Age (Ma)	Rb/Sr	$^{87}Sr/^{86}Sr$	$^{87}Sr/^{86}Sr_o$	$^{143}Nd/^{144}Nd$	$^{206}Pb/^{204}Pb$	$^{207}Pb/^{204}Pb$	$^{208}Pb/^{204}Pb$
Visegrád Mts									
PS4*	rhyodacite	15·7	0·454	0·71034	0·71004	0·51230	18·779	15·680	38·942
PS6*	rhyodacite	15·7	0·486	0·71036	0·71004	n.a.	n.a.	n.a.	n.a.
CS5*	rhyodacite	16·7	0·408	0·71002	0·70975	n.a.	n.a.	n.a.	n.a.
H1*	rhyodacite	16·7	0·370	0·71001	0·70977	0·51231	n.a.	n.a.	n.a.
K-L2*	rhyodacite	15·9	0·549	0·70996	0·70959	n.a.	n.a.	n.a.	n.a.
CSH*	dacite	16·5	0·314	0·70939	0·70918	0·51235	18·779	15·676	38·918
PS5	dacite	15·0	0·346	0·70977	0·70954	n.a.	n.a.	n.a.	n.a.
H2	andesite	16·5	0·218	0·70918	0·70904	n.a.	n.a.	n.a.	n.a.
L2	andesite	15·8	0·254	0·70933	0·70917	0·51233	n.a.	n.a.	n.a.
CS1	andesite	15·0	0·134	0·70899	0·70891	n.a.	n.a.	n.a.	n.a.
CS3A	andesite	15·0	0·184	0·70841	0·70830	n.a.	n.a.	n.a.	n.a.
12/1A	bas.and.	15·4	0·108	0·70751	0·70745	n.a.	n.a.	n.a.	n.a.
30/1	andesite	15·5	0·184	0·70719	0·70708	0·51246	18·795	15·674	38·926
30/2A	andesite	15·5	0·170	0·70756	0·70746	n.a.	n.a.	n.a.	n.a.
L84	andesite	16·5	0·174	0·70727	0·70717	n.a.	n.a.	n.a.	n.a.
A7	andesite	15·1	0·183	0·70798	0·70787	0·51240	n.a.	n.a.	n.a.
18/1	andesite	15·4	0·188	0·70778	0·70766	n.a.	n.a.	n.a.	n.a.
S3b	bas.and.	15·0	0·154	0·70768	0·70759	n.a.	n.a.	n.a.	n.a.
S4	andesite	15·0	0·217	0·70866	0·70854	0·51232	n.a.	n.a.	n.a.
S10	andesite	15·0	0·149	0·70745	0·70737	n.a.	n.a.	n.a.	n.a.
12/2A	andesite	15·8	0·120	0·70807	0·70800	0·51225	18·806	15·677	38·994
PR1	bas.and.	15·3	0·127	0·70709	0·70702	0·51242	18·914	15·682	39·030
Börzsöny									
B2L*	andesite	16·0	0·326	0·71011	0·70990	0·51234	18·806	15·679	38·967
L-NV*	dacite	16·0	0·297	0·71015	0·70996	0·51231	n.a.	n.a.	n.a.
B26*	dacite	16·0	0·294	0·71019	0·71000	n.a.	n.a.	n.a.	n.a.
B2/1	dacite	16·0	0·233	0·70863	0·70847	n.a.	n.a.	n.a.	n.a.
B7L	andesite	15·5	0·210	0·70832	0·70819	n.a.	n.a.	n.a.	n.a.
B24A	andesite	14·0	0·113	0·70695	0·70689	n.a.	n.a.	n.a.	n.a.
B-72	andesite	13·5	0·180	0·70845	0·70835	0·51241	18·916	15·676	38·992
B-3	andesite	13·5	0·164	0·70743	0·70734	0·51253	18·944	15·678	39·031
B-134	andesite	14·0	0·195	0·70854	0·70843	n.a.	n.a.	n.a.	n.a.
B-144	andesite	14·0	0·218	0·70910	0·70897	n.a.	n.a.	n.a.	n.a.
Central Slovakia									
S-B1*	andesite	16·00	0·225	0·70700	0·70685	0·51246	18·818	15·669	38·987
S-V1	andesite	16·00	0·209	0·70912	0·70898	0·51233	n.a.	n.a.	n.a.
S-V2	andesite	16·00	0·299	0·70895	0·70875	n.a.	n.a.	n.a.	n.a.
S-V4	andesite	16·00	0·251	0·71013	0·70996	0·51226	18·843	15·677	39·049
S-V5	andesite	16·00	0·290	0·70886	0·70867	n.a.	n.a.	n.a.	n.a.
S-P4	andesite	12·00	0·220	0·70759	0·70745	n.a.	n.a.	n.a.	n.a.
S-P5	andesite	15·00	0·205	0·70786	0·70772	0·51244	n.a.	n.a.	n.a.
SK3	andesite	16·00	0·226	0·70893	0·70878	0·51233	n.a.	n.a.	n.a.
SK9	rhyolite	11·50	1·489	0·70730	0·70650	0·51245	n.a.	n.a.	n.a.
S-P1	dacite	13·00	0·351	0·70827	0·70808	n.a.	n.a.	n.a.	n.a.
SK4	andesite	13·00	0·297	0·70532	0·70516	0·51263	n.a.	n.a.	n.a.
SK2	dacite	12·00	0·580	0·70772	0·70741	0·51239	n.a.	n.a.	n.a.
SK7	rhyolite	11·00	1·282	0·70635	0·70579	0·51258	n.a.	n.a.	n.a.
SK5	basalt	11·00	0·079	0·70478	0·70475	0·51268	19·186	15·676	39·178
SK8	basalt	11·00	0·102	0·70587	0·70583	0·51254	18·884	15·657	38·875

(continued)

Table 2: Continued

Sample	Rock type	Age (Ma)	Rb/Sr	$^{87}Sr/^{86}Sr$	$^{87}Sr/^{86}Sr_o$	$^{143}Nd/^{144}Nd$	$^{206}Pb/^{204}Pb$	$^{207}Pb/^{204}Pb$	$^{208}Pb/^{204}Pb$
Crustal xenoliths									
SCX-1	granite			0·70880		0·51228	n.a.	n.a.	n.a.
SCX-2	amphibolite			0·70770		0·51261	n.a.	n.a.	n.a.
SCX-3	gneiss			0·71248		0·51260	19·366	15·650	40·392
SCX-4	gneiss			0·70824		0·51293	n.a.	n.a.	n.a.
SCX-5	gneiss			0·70517		0·51284	n.a.	n.a.	n.a.
SCX-8	paragneiss			0·70796		0·51273	n.a.	n.a.	n.a.
SCX-10	gneiss			0·70566		0·51280	n.a.	n.a.	n.a.

Crustal xenoliths are from the garnet-bearing andesite of Siatoros (Karancs; Harangi *et al.*, 2001). Nd and Pb isotope data are not age-corrected because of the minor affect on the measured ratios. bas.and., basaltic andesite.
*Major and trace element data have been published by Harangi *et al.* (2001).

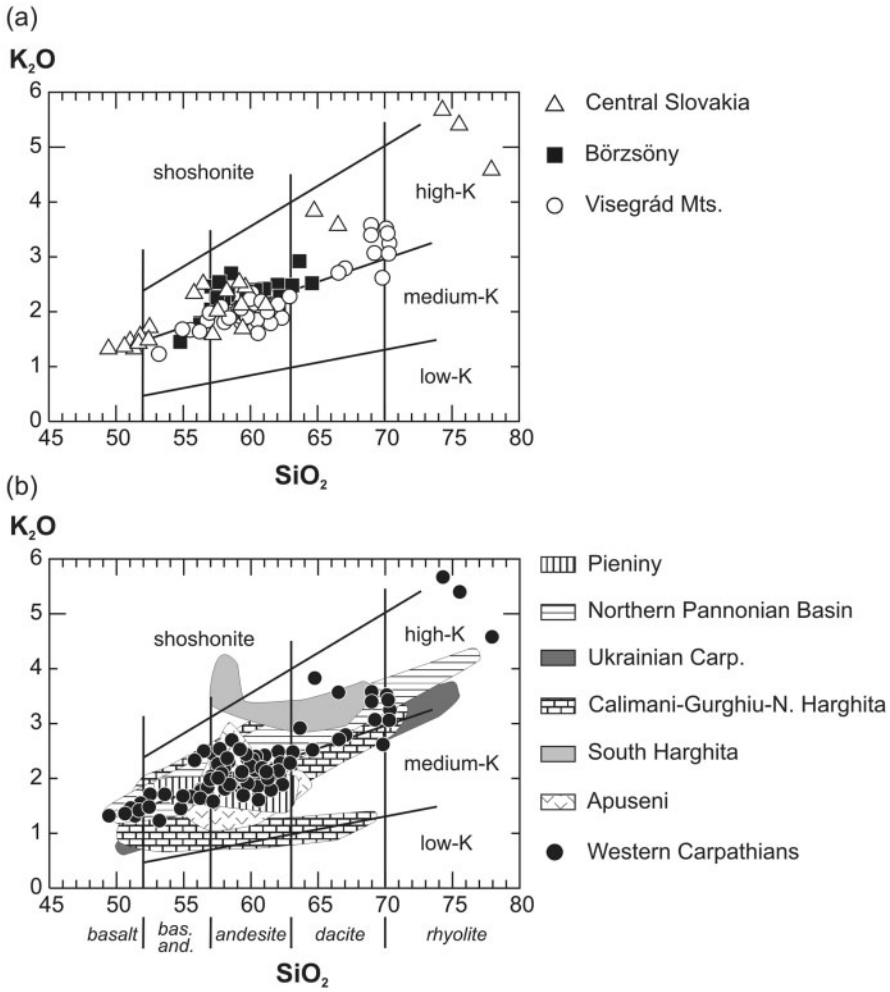

Fig. 3. (a) Classification of the calc-alkaline volcanic rocks of the three main parts of the WCVF based on the SiO_2 vs K_2O diagram (Peccerillo & Taylor, 1976). (b) Comparison of the WCVF volcanic rocks with those from the other Neogene to Quaternary calc-alkaline volcanic areas of the CPR. Pieniny: Trua *et al.* (2006); Ukrainian Carpathians: Seghedi *et al.* (2001); Calimani–Gurghiu–North Harghita: Mason *et al.* (1996); South Harghita: Mason *et al.* (1996) and Vinkler *et al.* (2007); Northern Pannonian Basin (Cserhát–Mátra–Tokaj–Slanec): Downes *et al.* (1995*a*). bas. and., basaltic andesite.

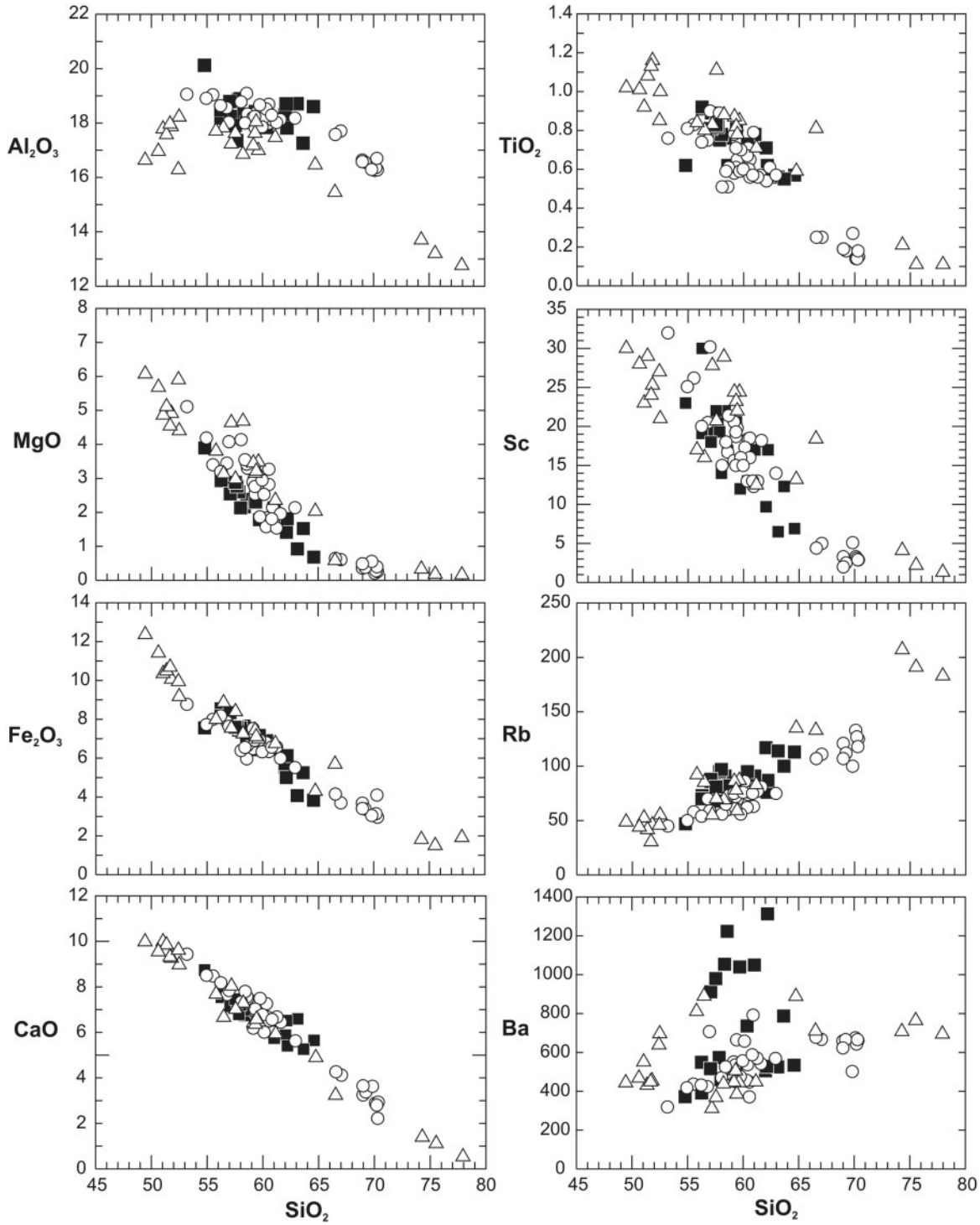

Fig. 4. Variation of selected major and trace elements with SiO_2 (wt %) content. (For explanation of the symbols see Fig. 3a.)

Slovakia are strongly potassic. In general, the WCVF rocks show less variation in K_2O at a given SiO_2 range than calc-alkaline rocks from the Eastern Carpathians (Fig. 3b). TiO_2, Fe_2O_3 and CaO decrease linearly with increasing SiO_2 in each suite (Fig. 4), whereas MgO shows a curvilinear trend. The Al_2O_3 content increases in the most mafic rocks and then decreases above 55 wt % SiO_2. Remarkably, samples

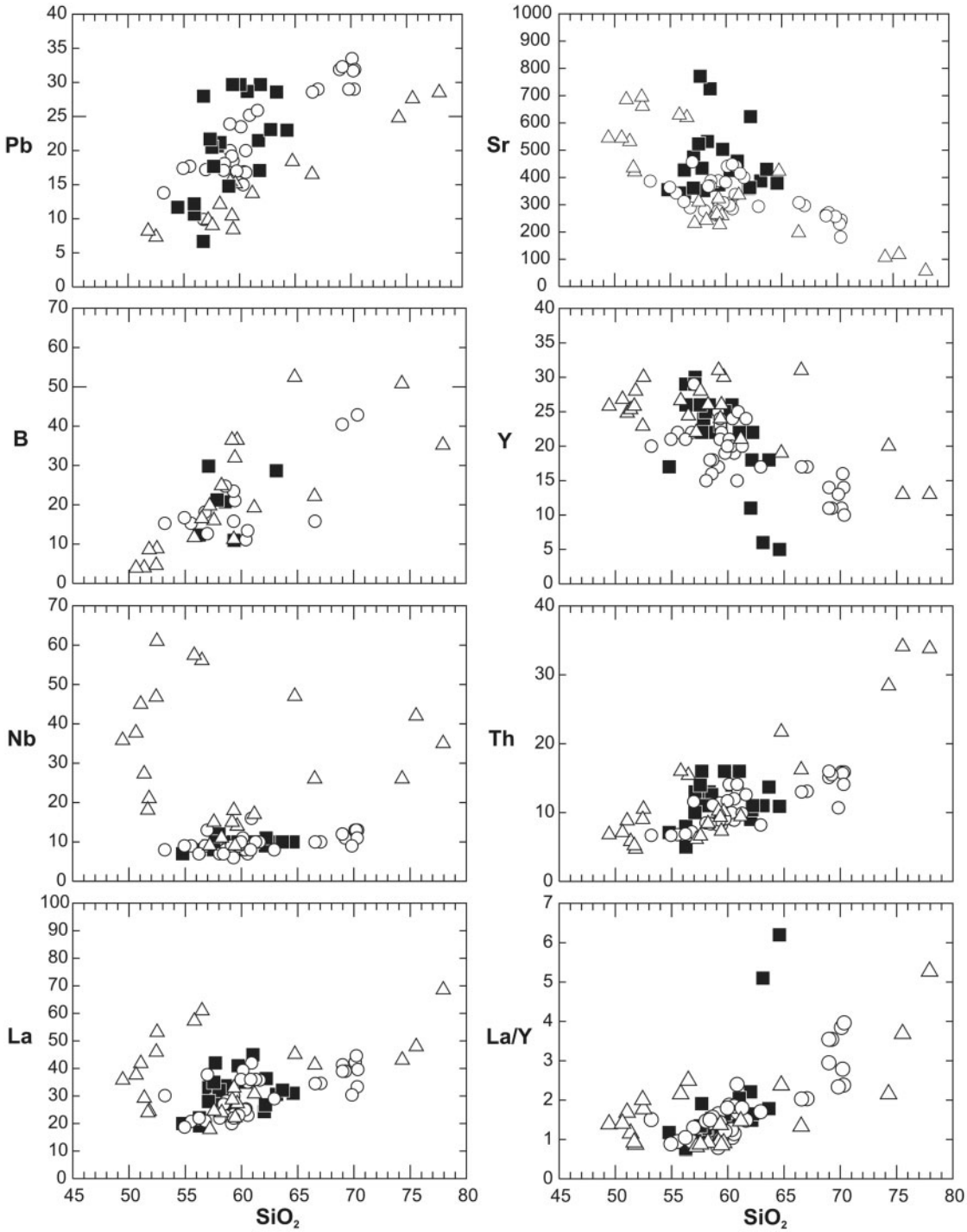

Fig. 4. Continued.

from central Slovakia have systematically lower Al_2O_3 and higher TiO_2 and MgO concentrations at a given SiO_2 content, compared with rocks from Visegrád and Börzsöny. This could indicate different parental magmas.

Strongly compatible trace elements such as Cr and Ni have low concentrations (Cr <60 ppm, Ni <15 ppm) in all samples including the most magnesian basalts, whereas Sc decreases linearly with increasing SiO_2 (Fig. 4). The LILE (e.g. Rb, Ba, Sr) and Pb usually show relatively large

scatter in the Harker diagrams (Fig. 4), except for Rb, which has a strong positive correlation with SiO_2. The K/Rb ratio is fairly constant (K/Rb = 200–280) throughout the sample set. Ba shows a complex variation with increasing SiO_2. The Börzsöny samples can be subdivided into two groups in terms of Ba (Fig. 4). The high Ba corresponds to an increase of other incompatible trace elements (both LILE and HFSE); therefore this could not be an alteration effect. Pb shows a positive correlation with SiO_2 content in the central Slovakian suite, whereas this correlation is much weaker in the Visegrád and Börzsöny samples (Fig. 4). In addition, the central Slovakian rocks contain typically less Pb at a given SiO_2 than samples from the southern areas. Boron concentrations show a wide range from 2 ppm to 50 ppm (Table 1; Gméling *et al.*, 2005, 2007) and correlate with the SiO_2 content. This range is similar that found in subduction-related volcanic rocks worldwide (Leeman & Sisson, 1996). The lowest B concentrations (2–10 ppm) are shown by the youngest basaltic rocks in central Slovakia.

In diagrams showing SiO_2 vs incompatible immobile trace elements (Fig. 4), the late-stage high-Al basalts deviate from the other rocks having significantly higher Nb and La contents. The La and Nb concentrations in these rocks correlate positively with SiO_2; however, both values increase rapidly within a relatively small SiO_2 range (49–56 wt %), which cannot be explained by pure fractional crystallization, but rather by different degrees of partial melting. The La/Nb ratio of these mafic rocks is fairly constant (1–1·3) and lower than in other WCVF rocks. Deviation of these rocks from the rest of the WCVF is underlined also by their La/Y vs SiO_2 trend. In general, the calc-alkaline rocks from central Slovakia have similar Th concentrations, but higher Nb and Y contents compared with samples from Visegrád and Börzsöny (Fig. 4). The Y concentration decreases abruptly above 62 wt % SiO_2. Depletion in Y and heavy REE (HREE) is especially typical of garnet-bearing dacites and rhyodacites in Visegrád and Börzsöny (Harangi *et al.*, 2001) and central Slovakian rhyolites.

The normal mid-ocean ridge basalt (N-MORB)-normalized trace element patterns and chondrite-normalized REE patterns of the WCVF volcanic rocks are shown in Fig. 5. The 15 Ma basaltic andesites have very uniform trace element patterns, enriched in LILE and showing a Nb trough and strong positive Pb anomaly, typical of subduction-related magmas (e.g. Ellam & Hawkesworth, 1988; Hawkesworth *et al.*, 1993; Pearce & Peate, 1995). In contrast, the late-stage (10 Ma) basalts show much less depletion in Nb (sometimes lacking Nb depletion entirely) and thus tend to resemble the later alkali basalts. These high-Al basalts also show strong light REE (LREE) enrichment and variable HREE contents. The andesites and dacites have very similar trace element patterns to the basaltic andesites, but with subtle variations in HREE values (Fig. 5). The rhyodacites and rhyolites show stronger enrichment in the incompatible trace elements compared with the andesites. Garnet-bearing rhyodacites have a pronounced depletion in Y and HREE, whereas the rhyolites are the only rock-types that show a negative Eu anomaly.

Sr–Nd–Pb isotopes

The Sr–Nd–Pb isotope compositions of the WCVF calc-alkaline volcanic rocks are given in Table 2. Initial $^{87}Sr/^{86}Sr$ and $^{143}Nd/^{144}Nd$ ratios show a wide range ($^{87}Sr/^{86}Sr = 0{\cdot}7048–0{\cdot}7100$; $^{143}Nd/^{144}Nd = 0{\cdot}51226–0{\cdot}51268$) but generally form a well-defined, curvilinear trend in a plot of $^{87}Sr/^{86}Sr$ vs $^{143}Nd/^{144}Nd$ (Fig. 6). This isotopic variation is similar to that of the wider range of Miocene calc-alkaline volcanic rocks in the Northern Pannonian Basin analysed by Salters *et al.* (1988), but differs from that of calc-alkaline rocks from the Eastern Carpathians (Mason *et al.*, 1996; Seghedi *et al.*, 2001) and from the Pieniny zone (Trua *et al.*, 2006). The post-extensional (11–0·2 Ma) alkali basalts of the Pannonian Basin continue this trend to higher $^{143}Nd/^{144}Nd$ and lower $^{87}Sr/^{86}Sr$ values, whereas the other end of the WCVF trend approaches the field of local crustal rocks and flysch sediments (Mason *et al.*, 1996). The WCVF data show a trend in isotopic composition with time; the early-stage (mainly garnet-bearing) rocks exhibit the highest $^{87}Sr/^{86}Sr$ and lowest $^{143}Nd/^{144}Nd$ values ($^{87}Sr/^{86}Sr = 0{\cdot}7095–0{\cdot}7105$ and $^{143}Nd/^{144}Nd = 0{\cdot}51226–0{\cdot}51235$) overlapping the isotopic ratios of the Early Miocene silicic volcanic rocks of the Pannonian Basin (Harangi, 2001). The 14–16 Ma andesites and dacites have a relatively small range of isotopic composition ($^{87}Sr/^{86}Sr = 0{\cdot}7065–0{\cdot}7083$; $^{143}Nd/^{144}Nd = 0{\cdot}51236–0{\cdot}51246$), whereas the youngest (<13 Ma) volcanic products show the highest $^{143}Nd/^{144}Nd$ and lowest $^{87}Sr/^{86}Sr$ values.

There is a much smaller variation in the Pb isotopes, especially in $^{207}Pb/^{204}Pb$ ratios (15·65–15·68), whereas the $^{206}Pb/^{204}Pb$ isotope ratios range from 18·77 to 19·19 (Fig. 6c). This isotopic range is smaller than that published previously by Salters *et al.* (1988) for a wider range of Northern Pannonian Basin calc-alkaline rocks, although this might be due to the more precise, double-spike lead isotope analysis performed in our study. The WCVF samples plot above the Northern Hemisphere Reference Line (NHRL; Hart, 1984); that is, they are relatively enriched in radiogenic ^{207}Pb, and plot slightly above the field of the alkali basalts of the Pannonian Basin. The Pb isotopes correlate with the temporal trend in Sr–Nd isotope ratios; that is, the lowest $^{206}Pb/^{204}Pb$ values characterize the oldest volcanic products, whereas the highest $^{206}Pb/^{204}Pb$ values are from the late-stage high-Al basalts from central Slovakia.

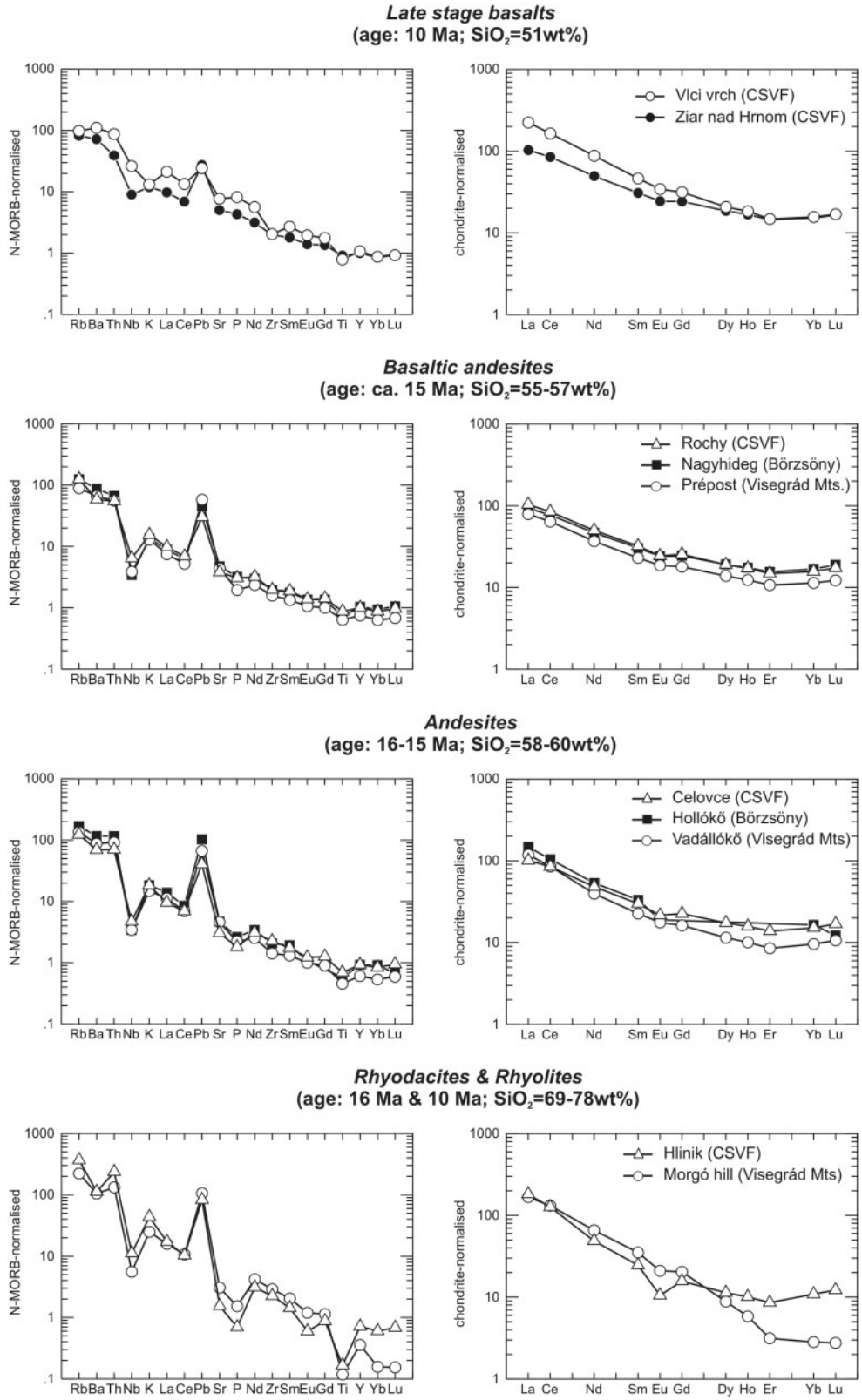

Fig. 5. N-MORB (Pearce & Parkinson, 1993) normalized trace element and chondrite (Sun & McDonough, 1989) normalized rare earth element patterns of the various rock types of the WCVF.

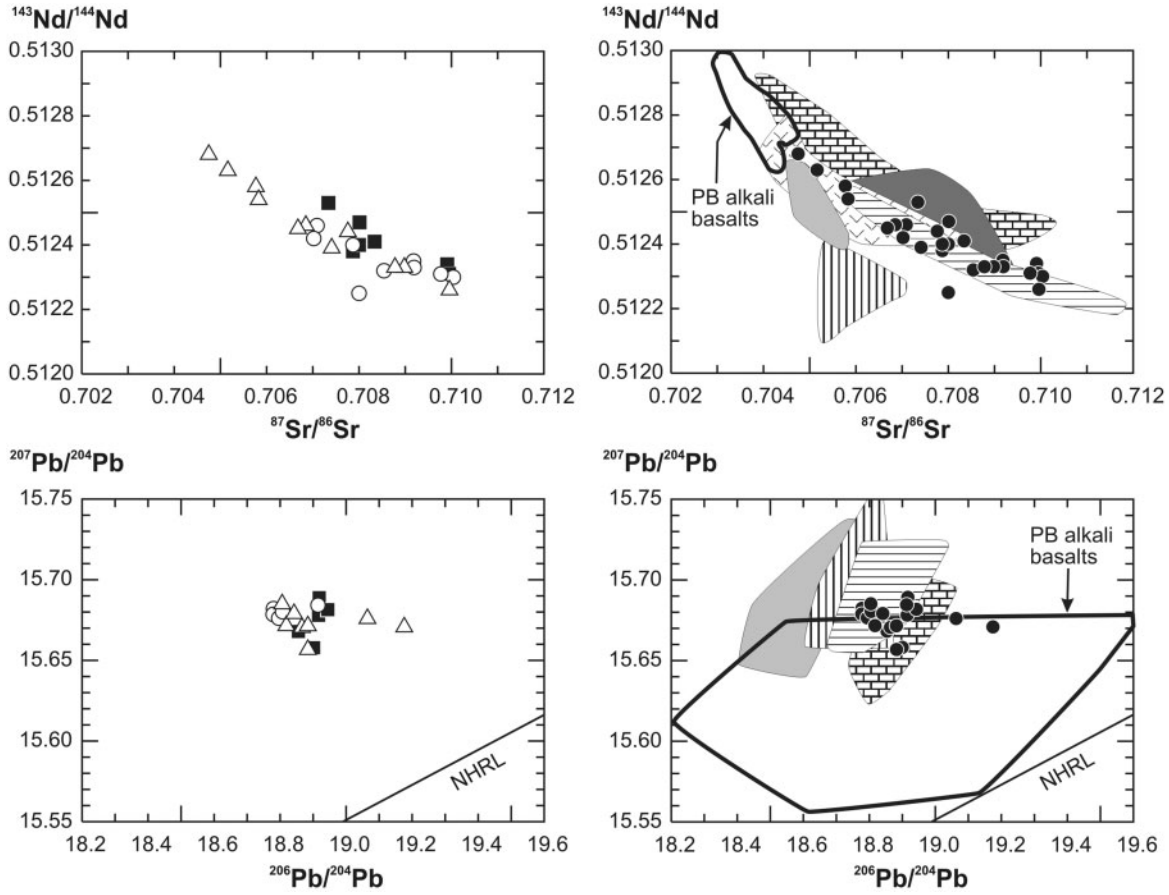

Fig. 6. Initial $^{87}Sr/^{86}Sr$ vs $^{143}Nd/^{144}Nd$ and $^{206}Pb/^{204}Pb$ vs $^{207}Pb/^{204}Pb$ for the WCVF calc-alkaline volcanic rocks and comparison with other Neogene to Quaternary calc-alkaline volcanic areas of the CPR. (For explanation of the symbols see Fig. 3.) NHRL, Northern Hemisphere Reference Line (Hart, 1984); PB, Pannonian Basin.

DISCUSSION

Shallow-level processes

The WCVF volcanic suites comprise mostly calc-alkaline andesites and dacites; basalts and basaltic andesites are rare and confined mostly to the later stages of magmatism. The andesites are rich in phenocrysts, such as plagioclase, amphibole, pyroxenes and rarely biotite, all showing disequilibrium features. Thus, shallow crustal processes must have had an important role in their petrogenetic evolution. Each volcano could have had its own complex magma plumbing system, although some common features can be recognized.

Garnet (almandine) phenocrysts occur only in the early andesites, dacites and rhyodacites (Harangi *et al.*, 2001). Amphiboles are also ubiquitous in these older rocks, whereas clino- and orthopyroxenes are more frequent in the younger rocks, implying a change from hydrous to anhydrous crystallization. The occurrence of primary almandines indicates crystallization at relatively high pressure (>7 kbar) and temperatures (900–950°C; Green, 1977, 1992). Almandine is not stable at shallow depths; hence a relatively rapid ascent of the host magma is necessary to preserve it in volcanic rocks (Fitton, 1972; Gilbert & Rogers, 1989). Almandines in andesites and dacites coexist with high-Al amphiboles (Al_2O_3 >12 wt %; Mg-hastingsites, pargasites), which could also have crystallized at high temperature and elevated pressure. High-Al amphibole megacrysts and amphibole-rich cognate xenoliths are often found in the andesites. They could have been picked up from deep-seated cumulates. In the post-16 Ma rocks, garnets are absent and the high-Al amphiboles are joined by low-pressure amphiboles. In many samples, both high- and low-Al amphiboles occur, suggesting mixing of crystal and liquid phases formed at various stages of differentiation as is common in arc rocks (Eichelberger, 1978; Dungan & Davidson, 2004; Davidson *et al.*, 2005). A plot of La/Y vs Y concentration (Fig. 7) shows the role of different minerals during magma differentiation. The samples form a curvilinear trend in this diagram. The relatively low Y concentration (<20 ppm) in the andesites can be explained by early crystallization of amphibole. This was followed by fractionation of plagioclase,

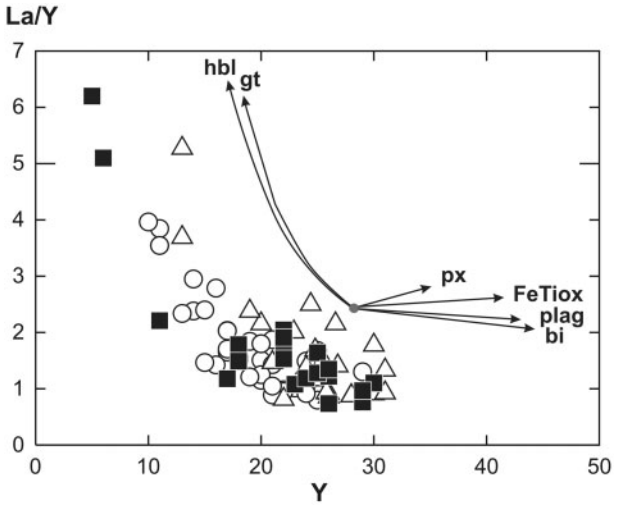

Fig. 7. Variation of La/Y vs Y for the WCVF samples explained by fractionation of various minerals (hbl, hornblende; gt, garnet; px, clino- and orthopyroxene; FeTiox, Ti-magnetite; plag, plagioclase; bi, biotite). Mineral vectors show the compositional change of the residual liquid after fractionation of 8% hornblende, 15% almandine garnet, 50% clino- or orthopyroxene, 50% Ti-magnetite, 50% plagioclase and 50% biotite, respectively. Mineral–liquid distribution coefficients are after Bacon & Druitt (1988), Green *et al.* (1989) and Ewart & Griffin (1994). It should be noted that the strong depletion in Y and the increase in the La/Y ratio can be explained also by the presence of residual garnet during the melt generation process. (For explanation of the symbols see Fig. 3a.)

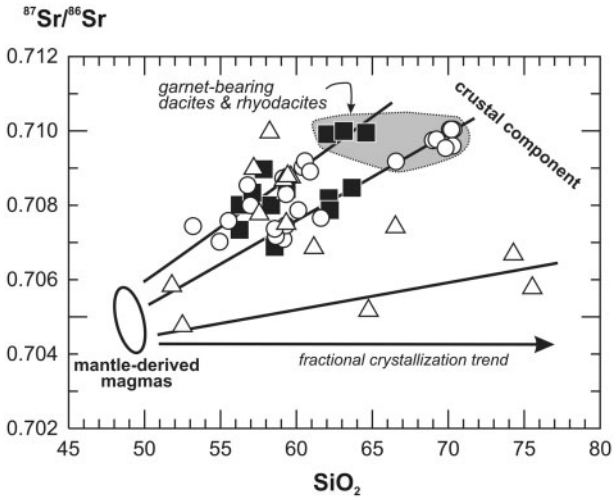

Fig. 8. SiO_2 vs $^{87}Sr/^{86}Sr$ for the WCVF calc-alkaline volcanic rocks. The positive correlation trends can be explained either by AFC processes or mixing between mantle-derived mafic magmas and silicic crustal melts, whereas the near-horizontal trend indicates closed-system fractional crystallization. The convergence of the trend lines, suggesting that parental magmas formed from a slightly heterogeneous mantle source, should be noted. (For explanation of the symbols see Fig. 3a.)

orthopyroxene, amphibole and magnetite in shallow-level magma chambers. The most extreme depletion in Y (<15 ppm) is shown by the garnet-bearing samples. High-pressure garnet fractionation could readily explain this bulk-rock composition, although the presence of residual garnet during the formation of the parental magmas cannot be excluded.

The basalts and basaltic andesites contain predominantly pyroxene phenocrysts, rather than amphibole. The youngest (11–12 Ma) basalts contain clinopyroxene with a systematically higher Ti and Al content than that in the older rocks. Olivine ($Fo_{60–80}$) phenocrysts occur sporadically in these mafic rocks. Evidence for mixing of crystal phases formed at different stages of magma evolution is also found in the most mafic rocks. Clinopyroxene (mg-number = 0·9) and amphibole (Al_2O_3 >15 wt %) megacrysts are common, probably derived from deep-seated cumulates.

Rhyolites were erupted roughly coeval with the youngest basalts at about 11–12 Ma. Lexa & Konečny (1998) and Konečny *et al.* (2002) interpreted these rocks as anatectic magmas formed by melting of lower crustal metagreywackes. However, these rhyolites have relatively low $^{87}Sr/^{86}Sr$ ratios (0·7057–0·7067), only slightly higher than those of the coeval basalts, so an assimilation–fractional crystallization (AFC) relationship between these two groups is more likely.

In summary, most of the WCVF volcanic rocks show clear evidence for shallow-level differentiation processes, such as crystal fractionation and crystal–melt hybridization. These processes can mask the original geochemical features of the magmas and thus make it difficult to have an insight into melt generation processes. Furthermore, the contribution of any crustal component also has to be evaluated before the nature of the magma source region can be discussed.

Crustal assimilation

Crustal involvement in WCVF magmagenesis is indicated by the relatively high $^{87}Sr/^{86}Sr$ and $^{207}Pb/^{204}Pb$ and low $^{143}Nd/^{144}Nd$ isotopic compositions of the magmatic rocks (Fig. 6). The crustal signature could be due to addition of subducted sediment to the mantle source region (source contamination) and/or to assimilation of crustal material during ascent of mantle-derived magma (crustal contamination; James, 1981; Davidson & Harmon, 1989).

The WCVF samples show a relatively large scatter in the SiO_2 vs $^{87}Sr/^{86}Sr$ diagram (Fig. 8), although a rough positive correlation can be observed. Increase of $^{87}Sr/^{86}Sr$ with SiO_2 as a differentiation index could indicate an AFC process, but could also be interpreted as a consequence of mixing between mantle-derived magmas and crustal melts. The data in Fig. 8. can be explained by a series of AFC trends with different assimilation rates and/or mixing with various crustal components. The model AFC–mixing trends converge to a possible mantle-derived

magma composition, which shows subtle $^{87}Sr/^{86}Sr$ isotope variation (from 0·704 to 0·7055). This may indicate derivation of the parental magmas from a slightly heterogeneous mantle source. The 11–12 Ma Central Slovakian basalt–rhyolite samples define a nearly horizontal trend, suggesting only a minor crustal signature and, possibly, a genetic link between the late-stage basaltic and rhyolitic magmas. In contrast, the other trends imply a fairly significant crustal component.

The highest $^{87}Sr/^{86}Sr$ values belong to the early garnet-bearing volcanic rocks (Fig. 8). These magmas cannot be the differentiation products of the andesitic melts, as they must have risen rapidly from lower crustal depths to preserve the early crystallized garnets. Furthermore, they are older than the andesites. The garnet-bearing dacites and rhyodacites show many petrological and geochemical similarities with the garnet- and cordierite-bearing dacites from the Betics of Spain (El Joyazo and Mazarrón areas; Zeck, 1970; Munksgaard, 1984; Cesare & Gómez-Pugnaire, 2001; Duggen *et al.*, 2005). The considerable involvement of crustal material is implied by the occurrence of Al-rich crustal xenoliths and garnet xenocrysts in both volcanic suites. Thus, melting of the lower crust has been suggested as an important role in their genesis (Zeck, 1970; Cesare & Gómez-Pugnaire, 2001; Harangi *et al.*, 2001). The xenocrystic garnets and the high-Al xenoliths point to a metasedimentary crustal source. Metasedimentary granulites form part of the lower crustal xenolith suite of the Pannonian Basin (Dobosi *et al.*, 2003; Embey-Isztin *et al.*, 2003; Török *et al.*, 2005). They have a mineral assemblage and geochemical composition suggesting a restitic origin. Török *et al.* (2005) proposed that significant melting in the lower crust could have occurred at the onset of lithospheric stretching (i.e. at 16–18 Ma). Garnets in the metasedimentary granulites have similar compositions to the xenocrystic almandines in the dacites, which could have been also restites incorporated into the silicic melts. The Sr–Nd–Pb isotopic composition of the metasedimentary granulites (Dobosi *et al.*, 2003) is roughly similar to that of the garnet-bearing dacites and rhyodacites.

A purely anatectic origin for the dacitic and rhyodacitic magmas is not, however, consistent with published data for the almandine phenocrysts, which are Ca-rich (CaO 4–8 wt %) and have relatively low $\delta^{18}O$ values (6·1–7·3‰). This indicates crystallization from a mantle-derived magma, whereas the xenocrystic almandines with lower Ca (CaO <2·5 wt %) and a $\delta^{18}O$ value of 10·5‰ (Harangi *et al.*, 2001) could be derived from the lower crust. These magmas were formed at the beginning of lithospheric extension of the Pannonian Basin, when the crust would have been significantly thicker (>40 km; Tari *et al.*, 1999). Thus, we suggest that mantle-derived mafic melts ponded beneath the thick continental crust and provided heat to generate silicic melt at the onset of lithospheric extension. The mafic and silicic magmas mixed thoroughly, resulting in dacitic–rhyodacitic magma compositions. Incorporation of S-type silicic melts increased the Al content of the hybrid magma, allowing crystallization of almandine at depth. The tensional stress field at the beginning of rifting presumably reactivated major faults, enhancing the rapid ascent of the silicic magmas. As the continental crust became thinner during the syn-rift phase (16–13 Ma), incorporation of lower crustal material into the mantle-derived magmas decreased significantly. Indeed, a gradual decrease in $^{87}Sr/^{86}Sr$ is observed in the younger andesites (Figs 6 and 8). Nevertheless, the isotope values of these rocks (e.g. $^{87}Sr/^{86}Sr = 0{\cdot}707–7085$) indicate that crustal contamination was still important in their genesis.

Implications for the nature of the mantle sources

The WCVF calc-alkaline rocks exhibit the typical geochemical characteristics of subduction-related magmas [elevated LILE, Pb and B concentrations, relative depletion in Nb, and high $^{87}Sr/^{86}Sr$ and $^{207}Pb/^{204}Pb$ and low $^{143}Nd/^{144}Nd$ (Figs 4–6)]. These features cannot be explained solely by assimilation of crustal material by mantle-derived magmas, but could indicate a source region metasomatized by aqueous fluids and/or melts derived from a subducted slab and subducted sediments (e.g. Tatsumi *et al.*, 1986; Hawkesworth *et al.*, 1993). Boron is a fluid-mobile and strongly incompatible trace element (having a very similar bulk distribution coefficient to Nb and La), which can be used to reveal the influence of slab-derived fluids in the magma source region (e.g. Morris *et al.*, 1990; Ryan & Langmuir, 1993; Ishikawa & Nakamura, 1994; Leeman *et al.*, 1994; Leeman & Sisson, 1996). The B/La and B/Nb ratios are dependant basically on fluid addition and do not change significantly during melting and magma differentiation. Pb and Ba are also mobile in aqueous fluids and thus Ba/La and Pb/La ratios are commonly used as indicators of aqueous fluid metasomatism. In Fig. 9, both the Slovakian and the Börzsöny–Visegrád samples show positive correlations between B/La and Pb/La, whereas Ba/La does not correlate with B/La. This suggests that Ba was not involved in the aqueous fluid metasomatism. Furthermore, the B/La and B/Nb ratios are relatively low. These trace element ratios appear to be diagnostic of the type of subduction. Low B/La and B/Nb ratios are found mostly in calc-alkaline volcanic rocks associated with shallow subduction of relatively warm, young oceanic lithospheres (Leeman *et al.*, 1994, 2004). Volcanic rocks from central and southern Italy show also low values of these ratios (Tonarini *et al.*, 2001, 2004), where melt generation is due to decompression

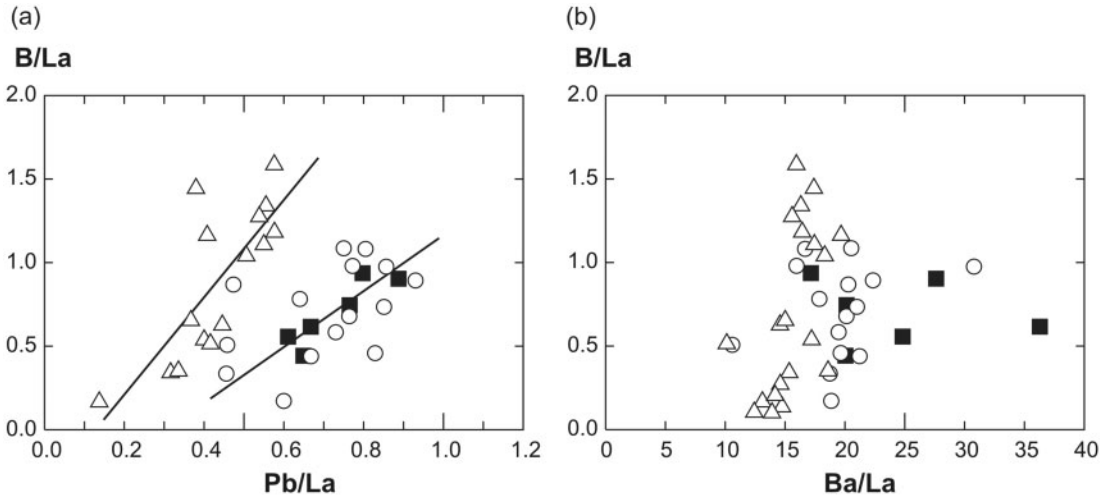

Fig. 9. Variation of B/La as a function of Pb/La and Ba/La. The B/La and Pb/La values show positive correlations (see linear regression lines) within the Slovakian and the Börzsöny–Visegrád samples, respectively. (For explanation of the symbols see Fig. 3.)

melting of subduction-related fluid-modified mantle (Peccerillo, 2005). In the CPR, subduction roll-back characterized Middle Miocene times with termination of active subduction north of the Western Carpathians. Thus, we may infer that the boron concentration data are consistent with a geodynamic setting similar to that of central and southern Italy.

Characterization of the nature of the mantle source before subduction–metasomatism is a challenging task in continental arc magmatism. Initial Sr–Nd–Pb isotope ratios depend on both the type of mantle source and the amount of incorporated crustal component. However, the $^{206}Pb/^{204}Pb$ ratio effectively distinguishes between the various mantle reservoirs, whereas the other isotope values can be used to infer the crustal component. In $^{206}Pb/^{204}Pb$–$^{87}Sr/^{86}Sr$–$^{143}Nd/^{144}Nd$ space, the WCVF samples define smooth curvilinear trends (Fig. 10). These trends are identical to those shown by other volcanic suites from the Central and Western Mediterranean (Vollmer, 1976; Gasperini *et al.*, 2002; Peccerillo, 2003; Duggen *et al.*, 2005) and can be interpreted as binary mixing hyperbolae between asthenospheric and crustal end-members. The mantle end-member is characterized by low $^{87}Sr/^{86}Sr$ and relatively high $^{206}Pb/^{204}Pb$ and $^{143}Nd/^{144}Nd$ values. This resembles the FOZO mantle reservoir as defined by Stracke *et al.* (2005) or the common European Asthenospheric Reservoir (Cebriá & Wilson, 1995; Hoernle *et al.*, 1995; Lustrino & Wilson, 2007). The crustal end-member is less well constrained. It could be lower or upper crust or subducted sediment. As discussed above, metasedimentary lower crustal material could play an important role in the genesis of the early stage WCVF calc-alkaline magmas. Assimilation of upper crustal material in the <15 Ma volcanic rocks can be also considered, particularly for those in Slovakia, where Hercynian granitic and metamorphic rocks occur in the basement (Tomek, 1993; Kohut *et al.*, 1999). However, the available Sr–Nd–Pb isotope data for these rocks (Kohut *et al.*, 1999; Poller *et al.*, 2005) do not support their involvement in the petrogenesis of the calc-alkaline magmas. Crustal xenoliths with a wide range of lithologies are fairly abundant in some of the WCVF volcanic rocks, but assimilation of these crustal lithologies by the ascending magmas can also be excluded based on their isotopic composition (Table 2). Crustal contamination could also occur, however, in the magma source region by metasomatism of the mantle via melt from subducted sediment. Mason *et al.* (1996) published isotope data for various flysch sediments from the Outer Carpathians. Some of these sediments could, potentially have been subducted and added to the mantle wedge. In the following model calculations (Table 3; Fig. 10), we consider both the incorporation of lower crustal materials into the magmas and source contamination processes. We use the isotopic compositions of metasedimentary granulite xenoliths from the Pannonian Basin (Dobosi *et al.*, 2003) to represent the lower crust and Cretaceous turbidite shale compositions (Mason *et al.*, 1996) to represent the subducted sediment.

Harangi (2001) used a simple binary mixing model to explain the isotope variation of the WCVF samples. We have modified this model, because it required mixing of >30% crustal component to form the late-stage WCVF basalts, which seems to be anomalously high. Instead, we prefer here a two-stage model (Fig. 10). In the first stage, an enriched asthenospheric (FOZO-like) mantle source is contaminated by melts derived from subducted sediment (mixing line A in Fig. 10). Approximately 1–2% of subducted sediment could have been added to the FOZO-like mantle, to form a metasomatized mantle source (metasomatized mantle1 in Fig. 10) that underwent further partial

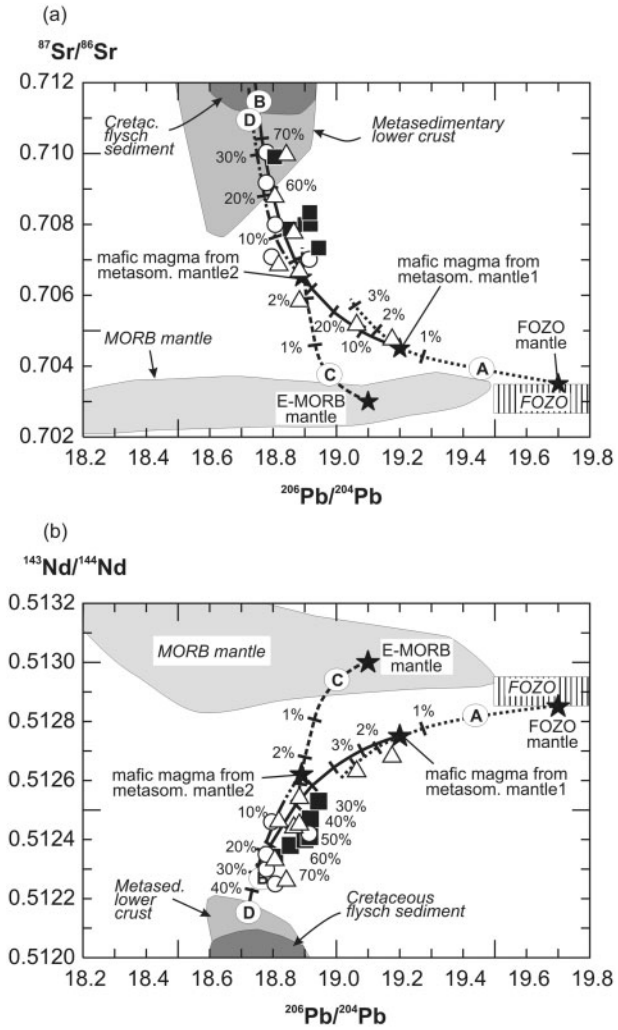

Fig. 10. Petrogenetic modelling for the genesis of the WCVF calc-alkaline rocks based on the variation of $^{87}Sr/^{86}Sr$, $^{143}Nd/^{144}Nd$ (both are sensitive to involvement of a crustal component) and $^{206}Pb/^{204}Pb$ (sensitive to the type of mantle component) isotope ratios. MORB mantle is based on the PETBD database (http://www.petdb.org/); FOZO is based on Stracke *et al.* (2005). The subducted sediment is modelled based on the composition of the Cretaceous flysch sediments found in the Eastern Carpathians (Mason *et al.*, 1996). Data for metasedimentary lower crust are from Dobosi *et al.* (2003). Explanation of the mixing trends is given in the text. (For explanation of the symbols see Fig. 3a.)

melting to produce the parental mafic magmas. The high $^{87}Sr/^{86}Sr$ of the WCVF samples indicates, however, involvement of additional crustal material. As discussed above, mafic magmas ponded at the crust–mantle boundary could have initiated melting in the overlying lower crust. Silicic melts from metasedimentary lower crustal material could have mixed with the mafic magmas derived from the metasomatized mantle (mixing line B in Fig. 10). At first the resulting dacitic–rhyodacitic melts could have contained as much as 60–70% of the lower crustal component, consistent with their slightly peraluminous character. Later, as the continental crust thinned, the fraction of the lower crustal component gradually decreased and the proportion of mantle-derived melt increased. This scenario is the simplest explanation for the isotopic variation of the WCVF volcanic rocks. However, we also test an alternative model with different mantle components. The isotopic composition of the older WCVF samples is not consistent with derivation from a depleted MORB-source mantle. Thus, in the second model, we consider an E-MORB-source mantle that was contaminated with 2–3% of subducted sediment (mixing line C in Fig. 10). The mafic melt formed from this metasomatized mantle source (metasomatized mantle2 in Fig. 10) mixed subsequently with the lower crustal component (mixing line D in Fig. 10). In this case, a smaller amount of crustal material (<30%) is required in the mixed magmas. This scenario could be applicable to the older (>15 Ma) magmatism of the Visegrád and Börzsöny Mts, but does not explain the genesis of the <15 Ma magmas in Central Slovakia. For this, a sharp change in composition of the mantle source is needed (i.e. from an E-MORB-type to a FOZO-type mantle). This change in the mantle source is reflected also in the trace element composition of the 11–12 Ma basalts (Figs 4 and 5). The elevated incompatible trace element concentrations and high La/Y ratio of these rocks indicate low-degree partial melting of an enriched mantle source. The isotopic variation of the post-15 Ma magmas can be explained by modification of a FOZO-like, enriched mantle by 1–2% subducted sedimentary component (trend A and metasomatized mantle1 in Fig. 10) followed by mixing of mafic melt derived from this metasomatized mantle with silicic melt from the metasedimentary lower crust (trend B in Fig. 10).

In both models, an enriched, FOZO-type mantle source, similar to that proposed for the Central and Western Mediterranean magmatism (Gasperini *et al.*, 2002; Peccerillo, 2003; Duggen *et al.*, 2005; Peccerillo & Lustrino, 2005; Lustrino & Wilson, 2007) played an important role in the genesis of the WCVF magmas. However, the location of this FOZO-like mantle is unclear. It could be related to mantle plume, but could also reside in the shallow heterogeneous mantle. In the next section, we discuss the role of this enriched mantle component in the genesis of the WCVF magmas and the relationships between the calc-alkaline magmatism and geodynamic processes such as subduction and extension.

Relationship between calc-alkaline magmatism and geodynamics

The WCVF volcanic suites exhibit many features in common with subduction-related volcanic rocks (Figs 5 and 6). Indeed, subduction has been generally regarded as an important process in the evolution of the CPR (Royden *et al.*, 1982; Csontos *et al.*, 1992; Tomek & Hall, 1993), although recent geophysical studies have

Table 3: Model parameters used in the petrogenetic modelling (Fig. 10)

	E-MORB mantle	FOZO mantle	Mafic magma from metasom. mantle1	Mafic magma from metasom. mantle2	Cretaceous flysch sediment (subducted sediment)	Metasedimentary lower crust
$^{87}Sr/^{86}Sr$	0·7030	0·7035	0·7045	0·7065	0·7200	0·7180
$^{143}Nd/^{144}Nd$	0·51300	0·51285	0·51275	0·51262	0·51210	0·51205
$^{206}Pb/^{204}Pb$	19·00	19·70	19·20	18·89	18·85	18·70
Sr	20	40	600	200	200	200
Nd	1·25	3	40	9	35	30
Pb	0·15	0·3	7	3	30	20

Trace elements are given in ppm; metasom., metasomatized. Metasomatized mantle1 and mantle2 are enriched mantle domains contaminated by subducted sediment.

questioned the southward subduction beneath the Western Carpathians (Grad *et al.*, 2006) and the westward subduction beneath the SE Carpathians (Knapp *et al.*, 2005). Nevertheless, most workers consider that subduction took place from the Late Cretaceous as recorded by the Cretaceous to Neogene flysch sediments around the present-day Carpathians (Horváth & Royden, 1981; Sandulescu, 1988; Csontos *et al.*, 1992). Approximately 260 km of shortening is estimated to have occurred in the Outer Carpathians from the Middle Oligocene to the Middle Miocene (Roure *et al.*, 1993; Behrmann *et al.*, 2000), coeval with extension of the Pannonian Basin (Royden *et al.*, 1983; Csontos *et al.*, 1992). Thus, the Carpathian volcanic arc has been commonly interpreted as a direct consequence of subduction (Bleahu *et al.*, 1973; Balla, 1981; Szabó *et al.*, 1992; Downes *et al.*, 1995a). However, there are some pecularities of the WCVF suite that may suggest a different magma-generation scenario.

During the first stage of volcanism (16·5–16 Ma), eruption of primary garnet-bearing magmas was coeval with the onset of rifting. Lithospheric stretching affected the WCVF area, as indicated by the relatively thin crust and lithosphere beneath this region (Horváth, 1993; Šefara *et al.*, 1996; Tari *et al.*, 1999) and the presence of syn-volcanic extensional structures in Central Slovakia (Nemčok & Lexa, 1990; Sperner *et al.*, 2002). Intermediate volcanism continued from 16·5 to 13 Ma, and eruption of a bimodal basalt–rhyolite suite took place at 12·5–11 Ma. This was followed by eruption of alkaline mafic magmas (Dobosi *et al.*, 1995) from 8 Ma to 0.2 Ma. A similar change from calc-alkaline to alkaline mafic magmatism has been described in many parts of the Mediterranean region and interpreted as the magmatic expression of the termination of subduction (e.g. Seyitoğlu *et al.*, 1997; Wilson *et al.*, 1997; El Bakkali *et al.*, 1998; Coulon *et al.*, 2002). However, subduction along the Western Carpathians was not contemporaneous with the calc-alkaline volcanism. Active subduction terminated north of the Western Carpathians at about 15–16 Ma, based on the age of the last thrust in the Outer Carpathians (Jiříček, 1979). Remarkably, active subduction was not associated with the calc-alkaline magmatism, which started just as active subduction ceased and lithospheric thinning commenced. Nevertheless, subduction of oceanic lithosphere may have continued at depth following continental collision in the upper crust. In this case, arc-type melts could have been generated in the mantle wedge as a result of the volatile flux from the descending slab, and the lithospheric extension only enhanced the ascent of the magmas. This scenario cannot be unambiguously excluded, although taking into account all the main features of the calc-alkaline magmatism described above, our suggestion is that extension and decompression melting of the passively upwelling, presumably metasomatized upper mantle could have primarily controlled the formation of magmas, as has been suggested for Western Anatolia (Seyitoğlu *et al.*, 1997; Wilson *et al.*, 1997) or the Basin and Range province, western USA (Hawkesworth *et al.*, 1995). Thus subduction played only an indirect role in magma generation.

A striking feature of the WCVF magmatism is the gradual change of magma composition; for example, La/Nb, Th/Nb and $^{87}Sr/^{86}Sr$ ratios decrease, whereas the $^{143}Nd/^{144}Nd$ and $^{206}Pb/^{204}Pb$ ratios increase with time (Harangi & Lenkey, 2007). In contrast, the Ba/La ratio and the $^{207}Pb/^{204}Pb$, $^{208}Pb/^{204}Pb$ isotope ratios do not show any clear temporal change. This compositional variation can be explained by a decreasing amount of the crustal component in the petrogenesis of the magmas and/or an increasing role of an enriched asthenospheric mantle source component. Both scenarios are consistent with magma generation beneath progressively thinning

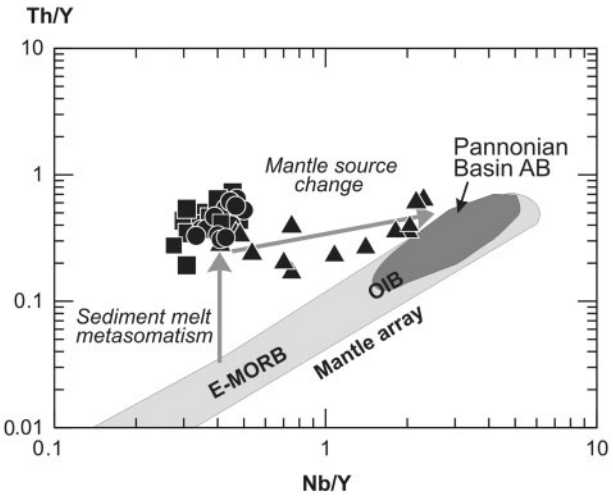

Fig. 11. Nb/Y vs Th/Y for the less evolved (MgO >3 wt %) calc-alkaline volcanic rocks of the WCVF. The elevated Th/Y ratio can be explained by addition of sedimentary melt to the source whereas the strong variation in the post-15 Ma rocks indicates change in the mantle source and involvement of increasing OIB-like mantle component. Pannonian Basin AB (alkaline basalts) are from Embey-Isztin *et al.* (1993), Dobosi *et al.* (1995), Downes *et al.* (1995*b*) and Harangi *et al.* (1995*a*). (For explanation of the symbols see Fig. 3a.)

lithosphere (crust and mantle). The change in the mantle source, that is, from a metasomatized E-MORB source mantle to a more enriched, ocean island basalt (OIB)-source (FOZO) mantle about 13–14 Ma, is clearly illustrated by a Nb/Y vs Th/Y diagram (Fig. 11). The appearance of the OIB-like, enriched mantle component in the late-stage calc-alkaline volcanism can be explained by various models such as: (1) mantle flow at a subducting slab edge as a result of roll-back; (2) formation of hot fingers in the mantle wedge; (3) retreating subduction at the eastern margin of the CPR initiating eastward mantle flow of the enriched asthenospheric mantle characteristic of western Europe; (4) delamination of the lower lithosphere and upwelling of hot asthenosphere (Seghedi *et al.*, 1998); (5) gradual slab detachment and deflection of upwelling mantle material from the NW (Harangi *et al.*, 2006); (6) back-arc type diapiric upwelling of the asthenosphere behind the active subduction zone (Konečny *et al.*, 2002); (7) progressive thinning of the continental lithosphere with a change of the mantle source region from the metasomatized lithospheric mantle to the underlying, passively upwelling asthenosphere.

A slab edge mantle flow model, such as that proposed for the South Sandwich arc–basin system (Leat *et al.*, 2004), is not consistent with the gradual temporal transition in magma composition. In addition, it would require a lateral change in magma composition that is not observed. Localized upwelling of hot asthenospheric material (hot fingers) along fractures within a curvilinear subducted slab could be another possible explanation, although we do not see a systematic distribution of the volcanoes (Tamura *et al.*, 2002) or a well-defined lateral compositional variation in the volcanic rocks. An alternative to this model could be the formation of a slab window and upwelling of deep mantle material through it, as proposed for the Central Italian magmatism by Gasperini *et al.* (2002). One problem with this model is, however, that a positive seismic velocity anomaly is observed beneath the CPR at 400–650 km depth (Wortel & Spakman, 2000; Piromallo *et al.*, 200l; Piromallo & Morelli, 2003). This has been interpreted as an accumulation of thick, cold material, possibly subducted residual lithosphere that would form a barrier against the rise of a lower mantle plume, and is also not consistent with shallow mantle plumes originating at the base of the upper mantle. During the Middle Miocene, subduction of oceanic lithosphere took place mostly in the Eastern Carpathians, whereas the Western Carpathian region was characterized by strike-slip faulting (Sperner *et al.*, 2002). Subduction roll-back played an important role in thinning the lithosphere and formation of the Pannonian Basin (Royden *et al.*, 1982; Csontos *et al.*, 1992). Retreating subduction could have initiated an eastward mantle flow (Doglioni, 1993). Assuming that the sub-lithospheric mantle beneath western and central Europe is characterized by a common enriched composition (Hoernle *et al.*, 1995), this eastward mantle flow could also provide an enriched mantle component beneath the Pannonian Basin. However, the geometry and temporal relationships of the calc-alkaline magmatism (Pécskay *et al.*, 2006) in the northern part of the Pannonian Basin, including the WCVF, do not seem to support a connection with eastward retreating subduction.

The other group of possible models emphasizes the post-collisional character of the calc-alkaline magmatism or the primary role of continental extension. Seghedi *et al.* (1998) explained the magmatism of the WCVF by subduction roll-back followed by lithospheric mantle delamination. Indeed, a slight northward migration of volcanic activity occurs within the WCVF and also in other volcanic complexes along the Northern Pannonian Basin. Lithospheric delamination can initiate upward asthenospheric flow and also partial melting of the delaminated and descending metasomatized lithospheric mantle. However, large-scale delamination would result in significant uplift of the area, which is not observed. Termination of active subduction is often accompanied by slab detachment, commonly considered to be an important process in the Mediterranean region (Wortel & Spakman, 2000); this has also been suggested for the northern part of the CPR during the Middle Miocene (Tomek & Hall, 1993). Slab detachment can also initiate mantle flow to fill the gap within the rifted subducted lithosphere (Davies & von Blanckenburg, 1995). Harangi *et al.* (2006) hypothesized that enriched

OIB-source mantle material from an assumed plume finger beneath the Bohemian Massif (Wilson & Patterson, 2001) could flow beneath the thinned lithosphere of the Pannonian Basin through the gap left behind by a detached slab under the western Carpathians. This could explain the appearance of such a mantle component at the end of the calc-alkaline magmatism (<13 Ma) and the subsequent alkaline mafic magmatism characterized by an isotopic signature akin to that of the European mafic rocks (Embey-Isztin *et al.*, 1993; Embey-Isztin & Dobosi, 1995). The drawback to this model is that plume activity is not proven beneath the Bohemian Massif and there is a lack of mantle anisotropy data beneath this region that could provide evidence for such a mantle flow.

Calc-alkaline magmatism could also take place as a response to lithospheric extension without contemporaneous subduction (Hawkesworth *et al.*, 1995; Hooper *et al.*, 1995; Wilson *et al.*, 1997; Fan *et al.*, 2003) and this has also been suggested for the WCVF magmatism by Lexa & Konečný (1974, 1998), Harangi (2001), Konečný *et al.* (2002) and Harangi & Lenkey (2007). This is consistent with the available structural data (Nemčok & Lexa, 1990; Tari *et al.*, 1999; Sperner *et al.*, 2002). In this scenario, the early stage (14–16 Ma) magmatism is the sign of the initiation of lithospheric thinning when partial melting took place in the lower part of the lithospheric mantle metasomatized by earlier subduction. The mafic magmas pond beneath the thick continental crust, resulting in melting of the lower crust. As lithospheric extension progresses, the crustal component decreases and the mantle source changes to a sub-lithospheric one.

CONCLUSIONS

The Carpathian–Pannonian region is a Mediterranean-type orogenic area characterized by various types of magmatic activity. One of its most prominent features is the development of a calc-alkaline volcanic chain along the inner Carpathian arc. Trace element and Sr–Nd–Pb isotopic data for Miocene (16·5–11 Ma) calc-alkaline volcanic rocks from the western segment of this volcanic arc (WCVF) provide an insight into the petrogenesis of these magmas and their geodynamic relationships. Crustal contamination played an important role in magma evolution, as in the Eastern Carpathians (Mason *et al.*, 1996). However, in the WCVF, involvement of lower crustal material is more pronounced. We propose that early mafic magmas ponded beneath the relatively thick continental crust and initiated melting in the lower crust. Mixing of silicic melts from metasedimentary lithologies with mafic magmas derived from the mantle resulted in hybrid dacitic magmas, from which almandine garnet crystallized at high pressure. Subsequently, as the continental crust thinned, the role of crustal contamination decreased. The WCVF calc-alkaline magmas show a gradual change of trace element and isotopic composition with time, consistent with a change of the magma source region, from an E-MORB-type mantle to a more enriched, OIB-type mantle. The latter has an isotopic character similar to FOZO as defined by Stracke *et al.* (2005) or the common European Asthenospheric Reservoir (Cebriá & Wilson, 1995; Hoernle *et al.*, 1995; Lustrino & Wilson, 2007). A plume origin for this mantle component is unlikely in the Pannonian Basin (Harangi & Lenkey, 2007). It could reside in the shallow asthenosphere and possibly also in the lower lithosphere, creating small-scale heterogeneity (Rosenbaum *et al.*, 1997). This magma generation model is strikingly different from that proposed for the East Carpathians by Mason *et al.* (1996). A change of mantle source can also be recognized in that magmatism (Mason *et al.*, 1998), from a depleted mantle source to a more enriched one, which yielded potassic magmas.

Transition from calc-alkaline to alkaline magmatism is observed in many parts of the Mediterranean region. We propose that this transition in the WCVF does not necessarily indicate a change in the geodynamic setting; that is, from subduction to extension. Instead, both types of magmatism are considered to be related to lithospheric extension. The calc-alkaline magmas were generated during the period of peak extension by melting of metasomatized lithospheric mantle and were contaminated by mixing with silicic lower crustal melts, whereas the later alkaline mafic magmas formed during the post-extensional stage by low-degree melting of the shallow asthenosphere.

ACKNOWLEDGEMENTS

Radiogenic isotope and X-ray fluorescence facilities at Royal Holloway were University of London Intercollegiate Research Services. We thank Gerry Ingram, Giz Marriner and Claire Grater for their assistance in the analytical work. Sz.H.'s research in London and Egham was supported by a NATO post-doctoral research fellowship from the Royal Society (1997–1998). This study was also supported by the Hungarian Science Foundation grant (OTKA T 037974) to Sz.H. K.G. would like to thank GVOP-3.2.1-2004-04-0268/3.0 for supporting the renovation of the detector; and NAP VENEUS05 Contract No. OMFB 00184/2006 for the improvement of the PGAA facility. Thorough reviews and detailed, constructive suggestions given by A. Peccerillo, M. Wilson, I. Seghedi and P. Macera helped us to clarify the ideas presented in this paper.

SUPPLEMENTARY DATA

Supplementary data for this paper are available at *Journal of Petrology* online.

REFERENCES

Agostini, S., Doglioni, C., Innocenti, F., Manetti, P., Tonarini, S. & Yilmaz Savaşçin, M. (2007). The transition from subduction-related to intraplate Neogene magmatism in the Western Anatolia and Aegean area. In: Beccaluva, L., Bianchini, G. & Wilson, M. (eds) *Cenozoic Volcanism in the Mediterranean Area. Geological Society of America, Special Paper* **418**, 1–15.

Aldanmaz, E., Pearce, J. A., Thirlwall, M. F. & Mitchell, J. G. (2000). Petrogenetic evolution of late Cenozoic, post-collision volcanism in western Anatolia, Turkey. *Journal of Volcanology and Geothermal Research* **102**, 67–95.

Bacon, C. R. & Druitt, T. H. (1988). Compositional evolution of the zoned calc-alkaline magma chamber of Mount Mazama, Crater Lake, Oregon. *Contributions to Mineralogy and Petrology* **98**, 224–256.

Baker, J. A., Menzies, M. A., Thirlwall, M. F. & Macpherson, C. G. (1997). Petrogenesis of Quaternary intraplate volcanism, Sana'a, Yemen: Implications for plume–lithosphere interaction and polybaric melt hybridization. *Journal of Petrology* **38**, 1359–1390.

Balla, Z. (1981). Neogene Volcanism of the Carpatho-Pannonian Region. *Earth Evolution Science* **3–4**, 240–248.

Behrmann, J. H., Staisny, S., Milicka, J. & Pereszlenyi, M. (2000). Quantitative reconstruction of orogenic convergence in the northeast Carpathians. *Tectonophysics* **319**, 111–128.

Birkenmajer, K., Trua, T., Serri, G. & Pécskay, Z. (2000). Geochemistry and K–Ar age of the Late Miocene intrusions, Pieniny Mts., Western Carpathians, Poland. *Vijesti Hrvatskoga Geološkog Društva* **37**, 25–26.

Bleahu, M., Boccaletti, M., Manetti, P. & Peltz, S. (1973). The Carpathian arc: A continental arc displaying the features of an 'island arc'. *Journal of Geophysical Research* **78**, 5025–5032.

Bourdon, B., Turner, S. & Dosseto, A. (2003). Dehydration and partial melting in subduction zones: Constraints from U-series disequilibria. *Journal of Geophysical Research B: Solid Earth* **108**, ECV 3-1–3-19.

Cameron, B. I., Walker, J. A., Carr, M. J., Patino, L. C., Matias, O. & Feigenson, M. D. (2003). Flux versus decompression melting at stratovolcanoes in southeastern Guatemala. *Journal of Volcanology and Geothermal Research* **119**, 21–50.

Cebriá, J. M. & Wilson, M. (1995). Cenozoic mafic magmatism in western/central Europe: A common European asthenospheric reservoir? *Terra Nova* **7**, 162.

Cesare, B. & Gómez-Pugnaire, M. T. (2001). Crustal melting in the Alboran domain: Constraints from xenoliths of the Neogene volcanic province. *Physics and Chemistry of the Earth, Part A: Solid Earth and Geodesy* **26**, 255–260.

Coulon, C., Megartsi, M. H., Fourcade, S., Maury, R. C., Bellon, H., Louni-Hacini, A., Cotten, J., Coutelle, A. & Hermitte, D. (2002). Post-collisional transition from calc-alkaline to alkaline volcanism during the Neogene in Oranie (Algeria): magmatic expression of a slab breakoff. *Lithos* **62**, 87–110.

Csontos, L., Nagymarosy, A., Horváth, F. & Kovac, M. (1992). Tertiary evolution of the Intra-Carpathian area: A model. *Tectonophysics* **208**, 221–241.

Davidson, J. P. & Harmon, R. S. (1989). Oxygen isotope constraints on the petrogenesis of volcanic arc magmas from Martinique, Lesser Antilles. *Earth and Planetary Science Letters* **95**, 255–270.

Davidson, J. P., Hora, J. M., Garrison, J. M. & Dungan, M. A. (2005). Crustal forensics in arc magmas. *Journal of Volcanology and Geothermal Research* **140**, 157–170.

Davies, J. H. & Von Blanckenburg, F. (1995). Slab breakoff: a model of lithosphere detachment and its test in the magmatism and deformation of collisional orogens. *Earth and Planetary Science Letters* **129**, 85–102.

Dobosi, G., Fodor, R. V. & Goldberg, S. A. (1995). Late-Cenozoic alkali basalt magmatism in Northern Hungary and Slovakia: petrology, source compositions and relationship to tectonics. In: Downes, H. & Vaselli, O. (eds) *Neogene and Related Magmatism in the Carpatho-Pannonian Region. Acta Vulcanologica* **7**, 199–207.

Dobosi, G., Kempton, P. D., Downes, H., Embey-Isztin, A., Thirlwall, M. F. & Greenwood, P. (2003). Lower crustal granulite xenoliths from the Pannonian Basin, Hungary, Part 2: Sr–Nd–Pb–Hf and O isotope evidence for formation of continental lower crust by tectonic emplacement of oceanic crust. *Contributions to Mineralogy and Petrology* **144**, 671–683.

Doglioni, C. (1993). Comparison of subduction zones versus the global tectonic pattern: a possible explanation for the Alps–Carpathians system. *Geophysical Transactions* **37**, 253–264.

Doglioni, C., Harabaglia, P., Merlini, S., Mongelli, F., Peccerillo, A. & Piromallo, C. (1999). Orogens and slabs vs their direction of subduction. *Earth-Science Reviews* **45**, 167–208.

Downes, H., Pantó, G., Póka, T., Mattey, D. & Greenwood, B. (1995*a*). Calc-alkaline volcanics of the Inner Carpathian arc, Northern Hungary: new geochemical and oxygen isotopic results. In: Downes, H. & Vaselli, O. (eds) *Neogene and Related Magmatism in the Carpatho-Pannonian Region. Acta Vulcanologica* **7**, 29–41.

Downes, H., Seghedi, I., Szakacs, A., Dobosi, G., James, D. E., Vaselli, O., Rigby, I. J., Ingram, G. A., Rex, D. & Pécskay, Z. (1995b). Petrology and geochemistry of late Tertiary/Quaternary mafic alkaline volcanism in Romania. *Lithos* **35**, 65–81.

Duggen, S., Hoernle, K., Bogaard, P., Rüpke, L. & Phipps-Morgan, J. (2003). Deep roots of the Messinian salinity crisis. *Nature* **422**, 602–606.

Duggen, S., Hoernle, K., van den Bogaard, P. & Garbe-Schönberg, D. (2005). Post-collisional transition from subduction-to intraplate-type magmatism in the westernmost Mediterranean: Evidence for continental-edge delamination of subcontinental lithosphere. *Journal of Petrology* **46**, 1155–1201.

Dungan, M. A. & Davidson, J. (2004). Partial assimilative recycling of the mafic plutonic roots of arc volcanoes: An example from the Chilean Andes. *Geology* **32**, 773–776.

Eichelberger, J. C. (1978). Andesitic volcanism and crustal evolution. *Nature* **275**, 21–27.

El Bakkali, S., Gourgaud, A., Bourdier, J.-L., Bellon, H. & Gundogdu, N. (1998). Post-collision Neogene volcanism of the Eastern Rif (Morocco): magmatic evolution through time. *Lithos* **45**, 523–543.

Ellam, R. M. & Hawkesworth, C. J. (1988). Elemental and isotopic variations in subduction related basalts: Evidence for a three component model. *Contributions to Mineralogy and Petrology* **98**, 72–80.

Elliott, T., Plank, T., Zindler, A., White, W. & Bourdon, B. (1997). Element transport from slab to volcanic front at the Mariana arc. *Journal of Geophysical Research* **102**, 14991–15019.

Embey-Isztin, A. & Dobosi, G. (1995). Mantle source characteristics for Miocene–Pleistocene alkali basalts, Carpathian–Pannonian Region: a review of trace elements and isotopic composition. In: Downes, H. & Vaselli, O. (eds) *Neogene and Related Volcanism in the Carpatho-Pannonian Region. Acta Vulcanologica* **7**, 155–166.

Embey-Isztin, A., Downes, H., James, D. E., Upton, B. G. J., Dobosi, G., Ingram, G. A., Harmon, R. S. & Scharbert, H. G. (1993). The petrogenesis of Pliocene alkaline volcanic rocks from the Pannonian Basin, Eastern Central Europe. *Journal of Petrology* **34**, 317–343.

Embey-Isztin, A., Downes, H., Kempton, P. D., Dobosi, G. & Thirlwall, M. F. (2003). Lower crustal granulite xenoliths from the Pannonian Basin, Hungary. Part l: mineral chemistry,

thermobarometry and petrology. *Contributions to Mineralogy and Petrology* **144**, 652–670.

Ewart, A. & Griffin, W. L. (1994). Application of proton-microprobe data to trace-element partitioning in volcanic rocks. *Chemical Geology* **117**, 251–284.

Fan, G., Wallace, T. C. & Zhao, D. (1998). Tomographic imaging of deep velocity structure beneath the Eastern and Southern Carpathians, Romania: implications for continental collision. *Journal of Geophysical Research* **103**, 2705–2723.

Fan, W.-M., Guo, F., Wang, Y.-J. & Lin, G. (2003). Late Mesozoic calc-alkaline volcanism of post-orogenic extension in the northern Da Hinggan Mountains, northeastern China. *Journal of Volcanology and Geothermal Research* **121**, 115–135.

Fitton, J. G. (1972). The genetic significance of almandine–pyrope phenocrysts in the calc-alkaline Borrowdale Volcanic Group, Northern England. *Contributions to Mineralogy and Petrology* **36**, 231–248.

Fodor, L., Csontos, L., Bada, G., Győrfi, I. & Benkovics, L. (1999). Tertiary tectonic evolution of the Pannonian basin system and neighbouring orogens: a new synthesis of palaeostress data. In: Durand, B., Jolivet, L., Horváth, F. & Séranne, M. (eds) *The Mediterranean Basins: Tertiary Extension within the Alpine Orogen. Geological Society, London, Special Publications* **156**, 295–334.

Gans, P. B., Mahood, G. A. & Schermer, E. (1989). Syn-extensional magmatism in the Basin and Range Province; A case study from the eastern Great Basin. *Geological Society of America, Special Papers* **233**, 53.

Gasperini, D., Blichert-Toft, J., Bosch, D., Del Moro, A., Macera, P. & Albarède, F. (2002). Upwelling of deep mantle material through a plate window: Evidence from the geochemistry of Italian basaltic volcanics. *Journal of Geophysical Research* **107**, 2367–2386.

Gilbert, J. S. & Rogers, N. W. (1989). The significance of garnet in the Permo-Carboniferous volcanic rocks of the Pyrenees. *Journal of the Geological Society, London* **146**, 477–490.

Gill, J. B. (1981). *Orogenic Andesites and Plate Tectonics*. Berlin.

Gill, J. B. & Williams, R. W. (1990). Th isotope and U-series studies of subduction-related volcanic rocks. *Geochimica et Cosmochimica Acta* **54**, 1427–1442.

Gméling, K., Harangi, S. & Kasztovszky, Z. (2005). Boron and chlorine concentration of volcanic rocks: An application of prompt gamma activation analysis. *Journal of Radioanalytical and Nuclear Chemistry* **265**, 201–212.

Gméling, K., Harangi, S. & Kasztovszky, Z. (2007). A bór geokémiai szerepe szubdukciós zónákban: A bór geokémiai változékonysága a Kárpát–Pannon térségben. (Geochemical importance of boron in subduction zones: Geochemical variation of boron in the Carpathian–Pannonian Region.) *Földtani Közlöny* (in press).

Grad, M., Guterch, A., Keller, G. R., Janik, T., Hegedűs, E., Vozár, J., Slaczka, A., Tiira, T. & Yliniemi, J. (2006). Lithospheric structure beneath trans-Carpathian transect from Precambrian platform to Pannonian basin: CELEBRATION 2000 seismic profile CEL05. *Journal of Geophysical Research B: Solid Earth* **111**, 1–23.

Granet, M., Wilson, M. & Achauer, U. (1995). Imaging a mantle plume beneath the French Massif Central. *Earth and Planetary Science Letters* **136**, 281–296.

Green, T. H. (1977). Garnet in silicic liquids and its possible use as a *P–T* indicator. *Contributions to Mineralogy and Petrology* **65**, 59–67.

Green, T. H. (1992). Experimental phase equilibrium studies of garnet-bearing I-type volcanics and high-level intrusives from Northland, New Zealand. *Transactions of the Royal Society of Edinburgh, Earth Sciences* **83**, 429–438.

Green, T. H., Sie, S. H., Ryan, C. G. & Cousens, D. R. (1989). Proton microprobe-determined partitioning of Nb, Ta, Zr, Sr and Y between garnet, clinopyroxene and basaltic magma at high pressure and temperature. *Chemical Geology* **74**, 201–216.

Grove, T. L. & Kinzler, R. J. (1986). Petrogenesis of andesites. *Annual Review of Earth and Planetary Sciences* **14**, 417–454.

Harangi, S. (2001). Neogene to Quaternary Volcanism of the Carpathian–Pannonian Region—a review. *Acta Geologica Hungarica* **44**, 223–258.

Harangi, S. & Lenkey, L. (2007). Genesis of the Neogene to Quaternary volcanism in the Carpathian–Pannonian region: Role of subduction, extension, and mantle plume. In: Beccaluva, L., Bianchini, G. & Wilson, M. (eds) *Cenozoic Volcanism in the Mediterranean Area. Geological Society of America, Special Paper* **418**, 67–92.

Harangi, S., Vaselli, O., Tonarini, S., Szabó, C., Harangi, R. & Coradossi, N. (1995*a*). Petrogenesis of Neogene extension-related alkaline volcanic rocks of the Little Hungarian Plain Volcanic Field (Western Hungary). In: Downes, H. & Vaselli, O. (eds) *Neogene and Related Magmatism in the Carpatho-Pannonian Region. Acta Vulcanologica* **7**, 173–187.

Harangi, S., Wilson, M. & Tonarini, S. (1995*b*). Petrogenesis of Neogene potassic volcanic rocks in the Pannonian Basin. In: Downes, H. & Vaselli, O. (eds) *Neogene and Related Magmatism in the Carpatho-Pannonian Region. Acta Vulcanologica* **7**, 125–134.

Harangi, S., Korpás, L. & Weiszburg, T. (1999). Miocene calc-alkaline volcanism of the Visegrád Mts., Northern Pannonian Basin. *Excursion Guide DMG-Tagung 1999 MinWien. Beihefte zum European Journal of Mineralogy* **11**, 7–20.

Harangi, S., Downes, H., Kósa, L., Szabó, C., Thirlwall, M. F., Mason, P. R. D. & Mattey, D. (2001). Almandine garnet in calc-alkaline volcanic rocks of the Northern Pannonian Basin (Eastern–Central Europe): geochemistry, petrogenesis and geodynamic implications. *Journal of Petrology* **42**, 1813–1843.

Harangi, S., Downes, H. & Seghedi, I. (2006). Tertiary–Quaternary subduction processes and related magmatism in the Alpine–Mediterranean region. In: Gee, D. & Stephenson, R. (eds) *European Lithosphere Dynamics. Geological Society, London, Memoirs* **32**, 167–190.

Hart, S. R. (1984). A large-scale isotope anomaly in the Southern Hemisphere mantle. *Nature* **309**, 753–757.

Hawkesworth, C. J., Gallagher, K., Hergt, J. M. & McDermott, F. (1993). Mantle and slab contributions in arc magmas. *Annual Review of Earth and Planetary Sciences* **21**, 175–204.

Hawkesworth, C., Turner, S., Gallagher, K., Hunter, A., Bradshaw, T. & Rogers, N. (1995). Calc-alkaline magmatism, lithospheric thinning and extension in the Basin and Range. *Journal of Geophysical Research* **100**, 10271–10286.

Hoernle, K., Zhang, Y. S. & Graham, D. (1995). Seismic and geochemical evidence for large-scale mantle upwelling beneath the eastern Atlantic and western and central Europe. *Nature* **374**, 34–39.

Hooper, P. R., Bailey, D. G. & McCarley Holder, G. A. (1995). Tertiary calc-alkaline magmatism associated with lithospheric extension in the Pacific Northwest. *Journal of Geophysical Research* **100**, 10303–10319.

Horváth, F. (1993). Towards a mechanical model for the formation of the Pannonian basin. *Tectonophysics* **226**, 333–357.

Horváth, F. (1995). Phases of compression during the evolution of the Pannonian Basin and its bearing on hydrocarbon exploration. *Marine and Petroleum Geology* **12**, 837–844.

Horváth, F. & Berckhemer, H. (1982). Mediterranean back arc basins. In: Berckhemer, H. & Hsü, K. (eds) *Alpine–Mediterranean Geodynamics. American Geophysical Union, Geodynamics Series* **7**, 141–173.

Horváth, F. & Cloetingh, S. (1996). Stress-induced late-stage subsidence anomalies in the Pannonian basin. *Tectonophysics* **266**, 287–300.

Horváth, F. & Royden, L. H. (1981). Mechanism for the formation of the intra-Carpathian basins: a review. *Earth Evolution Science* **3–4**, 307–316.

Ishikawa, T. & Nakamura, E. (1994). Origin of the slab component in arc lavas from across-arc variation of B and Pb isotopes. *Nature* **370**, 205–208.

Iwamori, H. (1998). Transportation of H_2O and melting in subduction zones. *Earth and Planetary Science Letters* **160**, 65–80.

James, D. E. (1981). The combined use of oxygen and radiogenic isotopes as indicators of crustal contamination. *Annual Review of Earth and Planetary Sciences* **9**, 311–344.

Jiříček, R. (1979). Tectonic development of the Carpathian arc in the Oligocene and Neogene. In: Mahel, M. (ed.) *Tectonic Profiles Through the West Carpathians*. Bratislava: Geologicky Ustav Dionyza Stura, pp. 205–214.

Johnson, R. W., Mackenzie, D. E. & Smith, I. E. M. (1978). Delayed partial melting of subduction-modified mantle in Papua New Guinea: 1. *Tectonophysics* **46**, 197–216.

Jolivet, L., Frizon de Lamotte, D., Mascale, A. & Séranne, M. (1999). The Mediterranean Basins: Tertiary extension within the Alpine orogen—an introduction. In: Durand, B., Jolivet, L., Horváth, F. & Séranne, M. (eds) *The Mediterranean Basins: Tertiary Extension within the Alpine Orogen. Geological Society, London, Special Publications* **156**, 1–14.

Karátson, D. (1995). Ignimbrite formation, resurgent doming and dome collapse activity in the Miocene Börzsöny Mountains, North Hungary. In: Downes, H. & Vaselli, O. (eds) *Neogene and Related Volcanism in the Carpatho-Pannonian Region. Acta Vulcanologica* **7**, 107–117.

Karátson, D., Márton, E., Harangi, S., Józsa, S., Balogh, K., Pécskay, Z., Kovácsvölgyi, S., Szakmány, G. & Dulai, A. (2000). Volcanic evolution and stratigraphy of the Miocene Börzsöny Mountains, Hungary: an integrated study. *Geologica Carpathica* **51**, 325–343.

Karátson, D., Oláh, I., Pécskay, Z., Márton, E., Harangi, S., Dulai, A. & Zelenka, T. (2007). Miocene volcanism in the Visegrád Mountains, Hungary: an integrated approach and regional implications. *Geologica Carpathica* (in press).

Knapp, J. H., Knapp, C. C., Raileanu, V., Matenco, L., Mocanu, V. & Dinu, C. (2005). Crustal constraints on the origin of mantle seismicity in the Vrancea Zone, Romania: The case for active continental lithospheric delamination. *Tectonophysics* **410**, 311–323.

Kohut, M., Kovach, V. P., Kotov, A. B., Salnikova, E. B. & Savatenkov, V. M. (1999). Sr and Nd isotope geochemistry of Hercynian granitic rocks from the Western Carpathians—implications for granite genesis and crustal evolution. *Geologica Carpathica* **50**, 477–487.

Konečný, V., Lexa, J. & Hojstricová, V. (1995). The Central Slovakia Neogene volcanic field: a review. In: Downes, H. & Vaselli, O. (eds) *Neogene and Related Magmatism in the Carpatho-Pannonian Region. Acta Volcanologica* **7**, 63–78.

Konečný, V., Kovác, M., Lexa, J. & Šefara, J. (2002). Neogene evolution of the Carpatho-Pannonian region: an interplay of subduction and back-arc diapiric uprise in the mantle. *Europeaan Geophysical Union, Stephan Mueller Special Publication Series* **1**, 105–123.

Kovac, M., Nagymarosy, A., Oszczypko, N., Slaczka, A., Csontos, L., Marunteanu, M., Matenco, L. & Márton, E. (1998). Palinspastic reconstruction of the Carpathian–Pannonian region during the Miocene. In: Rakús, M. (ed.) *Geodynamic Evolution of the Western Carpathians*. Bratislava: Geological Survey of Slovak Republik, pp. 189–217.

Leat, P. T., Pearce, J. A., Barker, P. F., Millar, I. L., Barry, T. L. & Larter, R. D. (2004). Magma genesis and mantle flow at a subducting slab edge: the South Sandwich arc–basin system. *Earth and Planetary Science Letters* **227**, 17–35.

Leeman, W. P. & Sisson, V. B. (1996). Geochemistry of boron and its implications for crustal and mantle processes. In: Anovitz, L. M. & Grew, E. S. (eds) *Boron: Mineralogy, Petrology and Geochemistry in the Earth's Crust. Mineralogical Society of America, Reviews in Mineralogy* **33**, 645–707.

Leeman, W. P., Carr, M. J. & Morris, J. D. (1994). Boron geochemistry of the Central American Volcanic Arc: Constraints on the genesis of subduction-related magmas. *Geochimica et Cosmochimica Acta* **58**, 149–168.

Leeman, W. P., Tonarini, S., Chan, L. H. & Borg, L. E. (2004). Boron and lithium isotopic variations in a hot subduction zone—the southern Washington Cascades. *Chemical Geology* **212**, 101–124.

Lenkey, L., Dövényi, P., Horváth, F. & Cloetingh, S. (2002). Geothermics of the Pannonian Basin and its bearing on the neotectonics. *European Geophysical Union Stephan Mueller Special Publications Series* **3**, 29–40.

Lexa, J. & Konečný, V. (1974). The Carpathian Volcanic Arc: a discussion. *Acta Geologica Hungarica* **18**, 279–294.

Lexa, J. & Konečný, V. (1998). Geodynamic aspects of the Neogene to Quaternary volcanism. In: Rakús, M. (ed.) *Geodynamic Development of the Western Carpathians*. Bratislava: Geological Survey of Slovak Republik, pp. 219–240.

Lustrino, M. (2000). Phanerozoic geodynamic evolution of the circum-Italian realm. *International Geology Review* **42**, 724–757.

Lustrino, M. & Wilson, M. (2007). The circum-Mediterranean anorogenic Cenozoic igneous province. *Earth-Science Reviews* **81**, 1–65.

Lustrino, M., Morra, V., Fedele, L. & Serracino, M. (2007). The transition between 'orogenic' and 'anorogenic' magmatism in the western Mediterranean area: The Middle Miocene volcanic rocks of Isola del Toro (SW Sardinia, Italy). *Terra Nova* **19**, 148–159.

Mason, P. R. D., Downes, H., Thirlwall, M. F., Seghedi, I., Szakács, A., Lowry, D. & Mattey, D. (1996). Crustal assimilation as a major petrogenetic process in east Carpathian Neogene to Quaternary continental margin arc magmas. *Journal of Petrology* **37**, 927–959.

Mason, P. R. D., Seghedi, I., Szakacs, A. & Downes, H. (1998). Magmatic constraints on geodynamic models of subduction in the East Carpathians, Romania. *Tectonophysics* **297**, 157–176.

Meulenkamp, J. E., Kovac, M. & Cicha, I. (1996). On Late Oligocene to Pliocene depocentre migrations and the evolution of the Carpathian–Pannonian system. *Tectonophysics* **266**, 301–317.

Morris, J. D., Leeman, W. P. & Tera, F. (1990). The subducted component in island arc lavas: Constraints from Be isotopes and B–Be systematics. *Nature* **344**, 31–36.

Munksgaard, N. C. (1984). High $\delta^{18}O$ and possible pre-eruptional Rb–Sr isochrons in cordierite-bearing Neogene volcanics from SE Spain. *Contributions to Mineralogy and Petrology* **87**, 351–358.

Nemčok, M. & Lexa, J. (1990). Evolution of the Basin and Range structure around the Ziar Mountain Range. *Geologica Carpathica* **41**, 229–258.

Nemčok, M., Hok, J., Kovac, P., Marko, F., Coward, M. P., Madaras, J., Houghton, J. J. & Bezak, V. (1998a). Tertiary extension development and extension/compression interplay in the West Carpathian mountain belt. *Tectonophysics* **290**, 137–167.

Nemčok, M., Pospisil, L., Lexa, J. & Donelick, R. A. (1998b). Tertiary subduction and slab break-off model of the Carpathian–Pannonian region. *Tectonophysics* **295**, 307–340.

Oncescu, M. C. & Bonjer, K. (1997). A note on the depth recurrence and strain release of large Vrancea earthquakes. *Tectonophysics* **272**, 291–302.

Oncescu, M. C., Burlacu, V., Anghel, M. & Smalberger, V. (1984). Three-dimensional P-wave velocity image under the Carpathian arc. *Tectonophysics* **106**, 305–319.

Pearce, J. A. (1982). Trace element characteristics of lavas from destructive plate boundaries. In: Thorpe, R. S. (ed.) *Andesites. Orogenic Andesites and Related Rocks*. Chichester: John Wiley, pp. 525–548.

Pearce, J. A. & Parkinson, I. J. (1993). Trace element models for mantle melting: application to volcanic arc petrogenesis. In: Prichard, H. M., Alabaster, T., Harris, N. B. W. & Neary, C. R. (eds) *Magmatic Processes and Plate Tectonics. Geological Society, London, Special Publications* **76**, 373–403.

Pearce, J. A. & Peate, D. W. (1995). Tectonic implications of the composition of volcanic arc magmas. *Annual Review of Earth and Planetary Sciences* **23**, 251–285.

Peccerillo, A. (2003). Plio-Quaternary magmatism in Italy. *Episodes* **26**, 222–226.

Peccerillo, A. (2005). *Plio-Quaternary Volcanism in Italy: Petrology, Geochemistry, Geodynamics*. Berlin: Springer.

Peccerillo, A. & Lustrino, M. (2005). Compositional variations of the Plio-Quaternary magmatism in the circum-Tyrrhenian area: deep- versus shallow-mantle processes. In: Foulger, G. R., Natland, J. H., Presnall, D. C. & Anderson, D. L. (eds) *Plates, Plumes and Paradigms. Geological Society of America, Special Papers* **388**, 421–434.

Peccerillo, A. & Taylor, S. R. (1976). Geochemistry of Eocene calc-alkaline volcanic rocks from the Kastamonu area, northern Turkey. *Contributions to Mineralogy and Petrology* **58**, 63–81.

Pécskay, Z., Lexa, J., Szakacs, A., Seghedi, I., Balogh, K., Konečný, V., Zelenka, T., Kovacs, M., Poka, T., Fulop, A., Marton, E., Panaiotu, C. & Cvetkovic, V. (2006). Geochronology of Neogene magmatism in the Carpathian arc and intra-Carpathian area. *Geologica Carpathica* **57**, 511–530.

Piromallo, C. & Morelli, A. (2003). P wave tomography of the mantle under the Alpine–Mediterranean area. *Journal of Geophysical Research* **108**, 2065doi:10.1029/2002JB001757.

Piromallo, C., Vincent, A. P., Yuen, D. A. & Morelli, A. (2001). Dynamics of the transition zone under Europe inferred from wavelet cross-spectra of seismic tomography. *Physics of the Earth and Planetary Interiors* **125**, 125–139.

Poller, U., Kohut, M., Gaab, A. S. & Todt, W. (2005). Pb, Sr and Nd isotope study of two coexisting magmas in the Nizke Tatry Mountains, Western Carpathians (Slovakia). *Mineralogy and Petrology* **84**, 215–231.

Ratschbacher, L., Frisch, W., Linzer, H.-G. & Marle, O. (1991). Lateral extrusion in the Eastern Alps, part 2: Structural analysis. *Tectonics* **10**, 257–271.

Rosenbaum, J. M., Wilson, M. & Downes, H. (1997). Multiple enrichment of the Carpathian–Pannonian mantle: Pb–Sr–Nd isotope and trace element constraints. *Journal of Geophysical Research* **102**, 14947–14962.

Roure, F., Roca, E. & Sassi, W. (1993). The Neogene evolution of the outer Carpathian flysch units (Poland, Ukraine and Romania): kinematics of a foreland/fold-and-thrust belt system. *Sedimentary Geology* **86**, 177–201.

Royden, L. H. (1993). Evolution of retreating subduction boundaries formed during continental collision. *Tectonics* **12**, 629–638.

Royden, L. H., Horváth, F. & Burchfiel, B. C. (1982). Transform faulting, extension and subduction in the Carpathian–Pannonian region. *Geological Society of America Bulletin* **93**, 717–725.

Royden, L. H., Horváth, F., Nagymarosy, A. & Stegena, L. (1983). Evolution of the Pannonian basin system. 2. Subsidence and thermal history. *Tectonics* **2**, 91–137.

Ryan, J. G. & Langmuir, C. H. (1993). The systematics of boron abundances in young volcanic rocks. *Geochimica et Cosmochimica Acta* **57**, 1489–1498.

Salters, V. J. M., Hart, S. R. & Pantó, G. (1988). Origin of Late Cenozoic volcanic rocks of the Carpathian arc, Hungary. In: Royden, L. H. & Horváth, F. (eds) *The Pannonian Basin. A Study in Basin Evolution. AAPG Memoirs* **45**, 279–292.

Sandulescu, M. (1988). Cenozoic tectonic history of the Carpathians. In: Royden, L. H. & Horváth, F. (eds) *The Pannonian Basin. AAPG Memoirs* **45**, 17–26.

Šefara, J., Bielik, M., Konečný, P., Bezak, V. & Hurai, V. (1996). The latest stage of development of the lithosphere and its interaction with the asthenosphere (Western Carpathians). *Geologica Carpathica* **47**, 339–347.

Seghedi, I., Balintoni, I. & Szakacs, A. (1998). Interplay of tectonics and neogene post-collisional magmatism in the intracarpathian region. *Lithos* **45**, 483–497.

Seghedi, I., Downes, H., Pécskay, Z., Thirlwall, M. F., Szakacs, A., Prychodko, M. & Mattey, D. (2001). Magmagenesis in a subduction-related post-collisional volcanic arc segment: the Ukrainian Carpathians. *Lithos* **57**, 237–262.

Seghedi, I., Downes, H., Szakacs, A., Mason, P. R. D., Thirlwall, M. F., Rosu, E., Pécskay, Z., Marton, E. & Panaiotu, C. (2004). Neogene–Quaternary magmatism and geodynamics in the Carpathian–Pannonian region: a synthesis. *Lithos* **72**, 117–146.

Seghedi, I., Downes, H., Harangi, S., Mason, P. R. D. & Pécskay, Z. (2005). Geochemical response of magmas to Neogene–Quaternary continental collision in the Carpathian–Pannonian region: A review. *Tectonophysics* **410**, 485–499.

Seyitoğlu, G. & Scott, B. C. (1992). Late Cenozoic volcanic evolution of the northeastern Aegean region. *Journal of Volcanology and Geothermal Research* **54**, 157–176.

Seyitoğlu, G., Anderson, D., Nowell, G. & Scott, B. (1997). The evolution from Miocene potassic to Quaternary sodic magmatism in western Turkey: implications for enrichment processes in the lithospheric mantle. *Journal of Volcanology and Geothermal Research* **76**, 127–147.

Simon, L. & Halouzka, R. (1996). Pútikov vrsok volcano—the youngest volcano in the Western Carpathians. *Slovak Geological Magazine* **2**, 103–123.

Spakman, W. (1990). Images of the upper mantle of central Europe and the Mediterranean. *Terra Nova* **2**, 542–553.

Sperner, B., Lorenz, F., Bonjer, K., Hettel, S., Muller, B. & Wenzel, F. (2001). Slab break-off—abrupt cut or gradual detachment? New insights from the Vrancea Region (SE Carpathians, Romania). *Terra Nova* **13**, 172–179.

Sperner, B., Ratschbacher, L. & Nemčok, M. (2002). Interplay between subduction retreat and lateral extrusion: Tectonics of the Western Carpathians. *Tectonics* **21**, 1.

Sperner, B., Ioane, D. & Lillie, R. J. (2004). Slab behaviour and its surface expression: New insights from gravity modelling in the SE Carpathians. *Tectonophysics* **382**, 51–84.

Stracke, A., Hofmann, A. W. & Hart, S. R. (2005). FOZO, HIMU, and the rest of the mantle zoo. *Geochemistry, Geophysics, Geosystems* **6**, paper number Q05007.

Sun, S.-S. & McDonough, W. F. (1989). Chemical and isotopic systematics of oceanic basalts: implications for mantle composition and processes. In: Saunders, A. D. & Norry, M. J. (eds) *Magmatism in the Ocean Basins. Geological Society, London, Special Publications* **42**, 313–345.

Szabó, C., Harangi, S. & Csontos, L. (1992). Review of Neogene and Quaternary volcanism of the Carpathian–Pannonian region. *Tectonophysics* **208**, 243–256.

Tamura, Y., Tatsumi, Y., Zhao, D., Kido, Y. & Shukuno, H. (2002). Hot fingers in the mantle wedge: new insights into magma genesis in subduction zones. *Earth and Planetary Science Letters* **197**, 105–116.

Tari, G., Dövényi, P., Horváth, F., Dunkl, I., Lenkey, L., Stefanescu, M., Szafián, P. & Tóth, T. (1999). Lithospheric structure of the Pannonian basin derived from seismic, gravity and geothermal data. In: Durand, B., Jolivet, L., Horváth, F. & Séranne, M. (eds) *The Mediterranean Basins: Tertiary Extension within the Alpine Orogen. Geological Society, London, Special Publications* **156**, 215–250.

Tatsumi, Y. (1989). Migration of fluid phases and genesis of basalt magmas in subduction zones. *Journal of Geophysical Research* **94**, 4697–4707.

Tatsumi, Y., Hamilton, D. L. & Nesbitt, R. W. (1986). Chemical characteristics of fluid phase released from a subducted lithosphere and origin of arc magmas: Evidence from high-pressure experiments and natural rocks. *Journal of Volcanology and Geothermal Research* **29**, 293–309.

Thirlwall, M. F. (1991). Long-term reproducibility of multicollector Sr and Nd isotope ratio analysis. *Chemical Geology* **94**, 85–104.

Thirlwall, M. F. (2000). Inter-laboratory and other errors in Pb isotope analyses investigated using a ^{207}Pb–^{204}Pb double spike. *Chemical Geology* **163**, 299–322.

Thomas, R. B., Hirschmann, M. M., Cheng, H., Reagan, M. K. & Edwards, R. L. (2002). ($^{231}Pa/^{235}U$)–($^{230}Th/^{238}U$) of young mafic volcanic rocks from Nicaragua and Costa Rica and the influence of flux melting on U-series systematics of arc lavas. *Geochimica et Cosmochimica Acta* **66**, 4287–4309.

Tomek, C. (1993). Deep crustal structure beneath the central and inner West Carpathians. *Tectonophysics* **226**, 417–431.

Tomek, C. & Hall, J. (1993). Subducted continental margin image din the Carpathians of Czechoslovakia. *Geology* **21**, 535–538.

Tonarini, S., Leeman, W. P. & Ferrara, G. (2001). Boron isotopic variations in lavas of the Aeolian volcanic arc, South Italy. *Journal of Volcanology and Geothermal Research* **110**, 155–170.

Tonarini, S., Leeman, W. P., Civetta, L., D'Antonio, M., Ferrara, G. & Necco, A. (2004). B/Nb and ^{11}B systematics in the Phlegrean Volcanic District, Italy. *Journal of Volcanology and Geothermal Research* **133**, 123–139.

Török, K., Dégi, J., Szép, A. & Marosi, G. (2005). Reduced carbonic fluids in mafic granulite xenoliths from the Bakony–Balaton Highland Volcanic Field, W Hungary. *Chemical Geology* **223**, 93–108.

Trua, T., Serri, G., Birkenmajer, K. & Pécskay, Z. (2006). Geochemical and Sr–Nd–Pb isotopic compositions of Mts Pieniny dykes and sills (West Carpathians): Evidence for melting in the lithospheric mantle. *Lithos* **90**, 57–76.

Turner, S., Regelous, M., Hawkesworth, C. & Rostami, K. (2006). Partial melting processes above subducting plates: Constraints from ^{231}Pa–^{235}U disequilibria. *Geochimica et Cosmochimica Acta* **70**, 480–503.

Turner, S. P., Platt, J. P., George, R. M. M., Kelley, S. P., Pearson, D. G. & Nowell, G. M. (1999). Magmatism associated with orogenic collapse of the Betic–Alboran Domain, SE Spain. *Journal of Petrology* **40**, 1011–1036.

Vinkler, A. P., Harangi, S., Ntaflos, T. & Szakács, A. (2007). A Csomád vulkán (Keleti Kárpátok) horzsaköveinek kozettani és geokémiai vizsgálata: petrogenetikai következtetések. *Földtani Közlöny* **137**, 103–128.

Vollmer, R. (1976). Rb–Sr and U–Th–Pb systematics of alkaline rocks: The alkaline rocks from Italy. *Geochimica et Cosmochimica Acta* **40**, 283–295.

Walsh, J. N., Buckley, F. & Barker, J. (1981). The simultaneous determination of the rare-earth elements in rocks using inductively coupled plasma source spectrometry. *Chemical Geology* **33**, 141–153.

Wilson, M. & Bianchini, G. (1999). Tertiary–Quaternary magmatism within the Mediterranean and surrounding regions. In: Durand, B., Jolivet, L., Horváth, F. & Séranne, M. (eds) *The Mediterranean Basins: Tertiary Extension within the Alpine Orogen. Geological Society, London, Special Publications* **156**, 141–168.

Wilson, M. & Downes, H. (1991). Tertiary–Quaternary extension-related alkaline magmatism in Western and Central Europe. *Journal of Petrology* **32**, 811–849.

Wilson, M. & Downes, H. (2006). Tertiary–Quaternary intra-plate magmatism in Europe and its relationship to mantle dynamics. In: Gee, D. & Stephenson, R. (eds) *European Lithosphere Dynamics. Geological Society, London, Memoirs* **32**, 147–166.

Wilson, M. & Patterson, R. (2001). Intraplate magmatism related to short-wavelength convective instabilities in the upper mantle: Evidence from the Tertiary–Quaternary volcanic province of western and central Europe. In: Ernst, R. E. & Buchan, K. L. (eds) *Mantle Plumes: Their Identification through Time. Geological Society of America, Special Papers* **352**, 37–58.

Wilson, M., Tankut, A. & Gulec, N. (1997). Tertiary volcanism of the Galatia province, north-west Central Anatolia, Turkey. *Lithos* **42**, 105–121.

Wortel, M. J. R. & Spakman, W. (2000). Subduction and slab detachment in the Mediterranean–Carpathian Region. *Science* **290**, 1910–1917.

Zeck, H. P. (1970). An erupted migmatite from Cerro del Hoyazo, SE Spain. *Contributions to Mineralogy and Petrology* **26**, 225–246.